The Role of Hypermutation and Collateral Sensitivity in Antimicrobial Resistance Diversity of *Pseudomonas aeruginosa* Populations in Cystic Fibrosis Lung Infection

Jelly Vanderwoude[1], Sheyda Azimi[1,2], Timothy D. Read[3] & Stephen P. Diggle[1*]

[1]Center for Microbial Dynamics and Infection, School of Biological Sciences, Georgia Institute of Technology, Atlanta, GA, USA; [2]School of Biology, Georgia State University, Atlanta, GA, USA; [3]Division of Infectious Diseases, Department of Medicine, Emory University School of Medicine, Atlanta, GA, USA

*Correspondence: stephen.diggle@biosci.gatech.edu

Preprint servers: This manuscript has been submitted as a preprint to bioRxiv

Keywords: cystic fibrosis; population heterogeneity; antibiotic resistance; hypermutation; evolution

Abstract

Pseudomonas aeruginosa is an opportunistic pathogen which causes chronic, drug-resistant lung infections in cystic fibrosis (CF) patients. In this study, we explore the role of genomic diversification and evolutionary trade-offs in antimicrobial resistance (AMR) diversity within *P. aeruginosa* populations sourced from CF lung infections. We analyzed 300 clinical isolates from four CF patients (75 per patient), and found that genomic diversity is not a consistent indicator of phenotypic AMR diversity. Remarkably, some genetically less diverse populations showed AMR diversity comparable to those with significantly more genetic variation. We also observed that hypermutator strains frequently exhibited increased sensitivity to antimicrobials, contradicting expectations from their treatment histories. Investigating potential evolutionary trade-offs, we found no substantial evidence of collateral sensitivity among aminoglycoside, beta-lactam, or fluoroquinolone antibiotics, nor did we observe trade-offs between AMR and growth in conditions mimicking CF sputum. Our findings suggest that (i) genomic diversity is not a prerequisite for phenotypic AMR diversity; (ii) hypermutator populations may develop increased antimicrobial sensitivity under selection pressure; (iii) collateral sensitivity is not a prominent feature in CF strains, and (iv) resistance to a single antibiotic does not necessarily lead to significant fitness costs. These insights challenge prevailing assumptions about AMR evolution in chronic infections, emphasizing the complexity of bacterial adaptation during infection.

Importance

Upon infection in the cystic fibrosis (CF) lung, *Pseudomonas aeruginosa* rapidly acquires genetic mutations, especially in genes involved in antimicrobial resistance (AMR), often resulting in diverse, treatment-resistant populations. However, the role of bacterial population diversity within the context of chronic infection is still poorly understood. In this study, we found that hypermutator strains of *P. aeruginosa* in the CF lung undergoing treatment with tobramycin evolved increased sensitivity to tobramycin relative to non-hypermutators within the same population. This finding suggests that antimicrobial treatment may only exert weak selection pressure on *P. aeruginosa* populations in the CF lung. We further found no evidence for collateral sensitivity in these clinical populations, suggesting that collateral sensitivity may not be a robust, naturally occurring phenomenon for this microbe.

Introduction

Pseudomonas aeruginosa is a dominant bacterial pathogen in chronic infections of the airways of adults with cystic fibrosis (CF), a genetic disorder that results in thickened mucus, persistent lung infection, and progressive decline in lung function [1, 2]. *P. aeruginosa* has multiple intrinsic and acquired mechanisms of antimicrobial resistance (AMR), with clinical strains sometimes displaying multi-drug resistance (MDR). While antibiotic treatment can be effective against early-stage, transient *P. aeruginosa* infections, in the case of chronic infections, antibiotic regimens ameliorate patient symptoms and prolong life but ultimately fail to eradicate *P. aeruginosa* from the CF lung [3]. This is largely due to the microaerophilic environment of the CF lung leading to slow growth and the viscous mucosal matrix hindering drug penetration [4, 5]. Treatment failure may additionally result from the high degree of phenotypic and genomic heterogeneity that naturally evolves in *P. aeruginosa* populations inhabiting CF airways [6], allowing the population to exploit various pathways of resistance and for the emergence of rare clones that evade treatment and re-establish infection afterwards [7, 8]. Most individuals with CF are initially infected by a single environmental or transmissible epidemic strain of *P. aeruginosa*, which then diversifies in the CF lung over the course of many years of infection [9]. Mutations in DNA mismatch repair (MMR) mechanisms act as a catalyst for this diversification, potentially providing an evolutionary advantage in an environment that demands rapid adaptation for survival, though potentially at a fitness cost [10, 11].

Maintaining diversity in populations can be advantageous for bet-hedging in a complex infection environment where there are a multitude of external stressors such as competing microbiota,

antibiotic exposure, and host immune responses. Heterogeneity in populations may develop as individual members of the population evolve specialized functions to occupy different ecological niches [12], however, adaptations to a particular niche may come at an expense to other energetically costly traits (i.e., fitness costs) [13, 14]. The vast diversity of *P. aeruginosa* in CF lung infection suggests that individual isolates within the population could have different specializations resulting in trade-offs with other traits. Of particular interest to researchers is collateral sensitivity— increased sensitivity to one antimicrobial as a trade-off with increased resistance to another— as a potential avenue for targeting drug-resistant populations using combination therapy or antibiotic cycling. Although collateral sensitivity has been evolved *in vitro* [15-19], it remains to be determined whether collateral sensitivity is robust across naturally occurring clinical populations of *P. aeruginosa*.

Despite *P. aeruginosa* population diversity in the CF lung being widely accepted, this diversity is often overlooked. Within-host adaptations of *P. aeruginosa* to the CF lung have previously been investigated and described, primarily via longitudinal single-isolate sampling [20-30]. Longitudinal sampling of single or small subsets of isolates from a population only reflects a fraction of the total evolutionary pathways exhibited within a population and may result in significant underestimation of the diversity of antimicrobial susceptibility profiles. As population diversity may impact infection outcomes via heteroresistance [31], microbial social interactions [32, 33], or the ability of a population to survive evolutionary bottlenecks [3], this warrants a shift in our sampling and susceptibility testing of chronic microbial infections to reflect our understanding of them as complex, dynamic populations. A few studies have thoroughly investigated population diversity in this infection context, in which their analyses were focused on (i) phenotypic diversity [34-38]; (ii) genetic analyses via pooled population sequencing [39, 40]; or (iii) both extensive sequencing and phenotyping, but lacking analysis linking the two at the isolate-level [6]. As a result, we still have an incomplete understanding of how genomic diversification drives AMR heterogeneity within a population, and what trade-offs are involved in these evolutionary processes.

Here, we investigated genomic and AMR diversity for chronic *P. aeruginosa* lung populations in four unique individuals with CF. We first sought to test whether genomic diversity is a strong predictor of phenotypic diversity in AMR within a population. With the rapid advances in sequencing technology, researchers are already investigating methods to replace time-consuming antimicrobial susceptibility testing (AST) with sequencing as a diagnostic tool [41]. As such, our goal was to determine the viability of predicting AMR phenotypic diversity from genomic

population diversity in a manner that could easily be translated to the clinic. We further explored the role that hypermutation plays in driving resistance, specific links between genotype and phenotype at the isolate-level, and enrichments in mutations and gene content changes relevant to AMR. Lastly, we searched for evidence that resistance to one antimicrobial may trade-off with sensitivity to other antimicrobials and fitness in a CF-like environment.

Methods

Cohort selection and strain isolation. We selected four adult individuals, aged 24-31 years, for this study from a cohort of CF patients at Emory University in Atlanta who had been chronically infected with *P. aeruginosa* for 10-15 years at the time of sampling. From each patient, we collected and processed a single expectorated sputum sample. We processed sputum by supplementing each sample with 5 ml synthetic cystic fibrosis medium (SCFM) [42] and autoclaved glass beads, homogenizing the mixture via vortexing for 2 mins, centrifuging the homogenized sputum mixture for 4 mins at ~3,300 x *g*, removing the supernatant, and conducting a 10x serial dilution of cell pellet re-suspended in phosphate buffered saline to streak on *Pseudomonas* isolation agar (PIA) plates. These plates were incubated at 37°C overnight, then at room temperature for up to 72 h. From each expectorated sputum sample, we randomly isolated 75 *P. aeruginosa* colonies for a total of 300 isolates. These isolates were confirmed to be *P. aeruginosa* using 16S rRNA gene amplification before proceeding with whole genome sequencing.

Whole genome sequencing. To conduct sequencing, we first grew all 300 isolates overnight in 15 ml conical tubes in lysogeny broth (LB) at 37°C with shaking at 200 rpm. We extracted DNA from these cultures using the Promega Wizard Genomic DNA Purification Kit according to the manufacturer's instructions. We prepared sequencing libraries using the Nextera XT DNA Library Preparation Kit and used the Illumina Novaseq platform to obtain 250 bp paired-end reads for a mean coverage of 70x. 28 samples either failed or did not meet the minimum sequencing coverage or quality requirements, so we re-sequenced these using the Illumina MiSeq platform for 250 bp paired-end reads and combined the reads from both sequencing runs to analyze these 28 samples. We randomly selected one isolate from each patient to serve as the reference strain for the other 74 isolates isolated from that patient. For these reference isolates, we additionally obtained Oxford Nanopore long read sequences through the Microbial Genome Sequencing

142 Center (GridION Flow Cell chemistry type R9.4.1 with Guppy high accuracy base calling v4.2.2)
143 at 35x coverage.
144
145 **Multi-locus sequence typing.** Our multi-locus sequence typing was implemented in Bactopia
146 v1.6.5 [43], which employs the PubMLST.org schema [44].
147
148 **Constructing annotated reference assemblies.** We used Unicyler v0.5.0 [45] to create long-
149 read assemblies for the four reference isolates. We then conducted one round of long-read
150 polishing on these assemblies using Medaka v1.0.3 [46], which produced preliminary consensus
151 sequences. We conducted quality control on all 300 Illumina reads using the Bactopia v1.6.5 [43]
152 pipeline. We conducted two further short-read assembly polishing steps on the long-read
153 assemblies by aligning the quality-adjusted short reads of each of the four reference isolates to
154 its respective consensus sequence using Polypolish v0.5.0 [47] and Pilon v1.24 [48]. We validated
155 the final consensus sequences by mapping the Illumina reads of each reference to its respective
156 assembly using Snippy v4.6.0 [49] and confirming that 0 variants were called. We used (i) Prokka
157 v1.14.6 [50] and (ii) RATT v1.0.3 [51] to (i) annotate our reference strains using a *P. aeruginosa*
158 pan-genome database collated by Bactopia, and to (ii) transfer gene annotations from PAO1 to
159 their respective positions in each of the reference strains, respectively.
160
161 **Variant calling.** We used Snippy v4.6.0 (39) to call variants from the other 296 isolates against
162 their respective reference strain and create a core genome alignment. Using PhyML
163 v3.3.20211231 (43), we created a maximum likelihood phylogeny. Then, using VCFtools v0.1.16
164 (44) and Disty McMatrixface v0.1.0 (45), we generated a pairwise SNP matrix for each patient.
165 For Disty, we only considered alleles in the core genome and chose to ignore ambiguous bases
166 pairwisely (-s 0). We then employed SnpEff and SnpSift v4.3t (46) to identify the affected genes
167 and sort the variants by predicted effect. We identified hypermutators in these populations by the
168 presence of non-synonymous mutations in *mutL*, *mutS*, and *uvrD* [52].
169
170 **Antimicrobial susceptibility testing.** To assess antimicrobial susceptibility profiles, we followed
171 the guidelines and standards provided by the Clinical and Laboratory Standards Institute (CLSI)
172 *Performance Standards for Antimicrobial Susceptibility Testing M100S*, 30th edition. We first grew
173 all isolates overnight in LB in 24-well microtiter plates at 37°C with shaking at 200 rpm. We diluted
174 cultures to a Macfarland standard of 0.5 (OD_{600} ~0.06) and streaked a lawn on 100x15 mm Petri

175 dishes with 20 ml Mueller-Hinton agar using pre-sterilized cotton swabs. We then stamped
176 amikacin (AK), meropenem (MEM), piperacilin-tazobactam (TZP), ciprofloxacin (CIP), tobramycin
177 (TOB), and ceftazidime (CAZ) on each plate and incubated for 17 h at 37°C. We measured the
178 zone of inhibition (ZOI) at 17 h and classified the values as resistant, intermediate, or susceptible
179 per the established CLSI interpretive criteria. We used *P. aeruginosa* strain ATCC 27853 as a
180 quality control. We tested all isolates in biological triplicates. We ran a Mann-Whitney U test to
181 compare the means of antimicrobial susceptibilities between hypermutators and normomutators
182 (non-hypermutators) and a Pearson's correlation coefficient to determine relationships between
183 susceptibilities to different antimicrobials, both using α = .05.

184

185 **Principal components analysis.** We conducted a principal components analysis of the
186 antimicrobial susceptibility data in R v4.3.0 using a singular value decomposition approach.

187

188 **Resistome genotyping.** We assessed genotypes relevant to resistance by uploading the *de*
189 *novo* assemblies to the Resistance Gene Identifier (RGI) v6.1.0 web portal, which predicts
190 resistomes using the Comprehensive Antibiotic Resistance Database (CARD) v3.2.6 [53]. We
191 excluded loose and nudge hits from this analysis.

192

193 **Enrichment analysis.** We conducted an enrichment analysis to determine which functional
194 categories of genes were differentially impacted by mutations than would be expected by random
195 chance. We used an in-house Python script to retrieve the PseudoCAP functional group of each
196 gene where a non-synonymous SNP or microindel was identified. We accounted for the varying
197 lengths of genes in each functional category in our analysis, based off their lengths and
198 prevalence in the PAO1 genome. We used a chi-squared goodness of fit test to conduct the
199 enrichment analyses for Patients 1-3 to determine which functional categories were
200 disproportionately impacted by non-synonymous variants. We used the R package XNomial
201 v1.0.4 [54] to conduct an exact multinomial goodness of fit test using Monte-Carlo simulations for
202 Patient 4 because the SNP frequencies of Patient 4 did not meet the assumptions for a chi-
203 squared test. Given the formula for calculating the chi-squared statistic: $\chi^2 = \sum \frac{(O-E)^2}{E}$, if the
204 $\frac{(O-E)^2}{E}$ value for a particular PseudoCAP functional category was in the top 30 percentile of all
205 values (top 8 of 27 total categories) in the analyses of at least three patients, we noted this as an
206 enrichment.

207
208 **Predicting putative recombination events.** We input the core genome alignment from each
209 patient to Gubbins v3.3.0 [55] to predict potential recombinant regions in each population.
210
211 **Analyzing growth curves.** To assess growth, we cultured strains for 24 h in 96-well microtiter
212 plates (Corning) at 37°C static, in 200µL synthetic cystic fibrosis sputum medium (SCFM) [42],
213 shaking for 4 s before reading optical density at 600 nm every 20 min. We tested all clinical
214 isolates in biological triplicates. We used GrowthCurver [56] to analyze the resulting growth curves
215 and calculate growth rate (r). We then assessed the relationship between growth rate and
216 susceptibility profiles using a linear mixed model in brms [57].
217
218 **Visualizations.** We conducted graphical analyses in R v4.3.0.
219
220 **Data availability.** The sequences in this study will be made available in the NCBI SRA database
221 upon publication.
222
223 **Results**
224 **Description of the four patient cohort selected for this study.** The four individuals selected
225 for this study were aged 24-31 years and had been chronically infected with *P. aeruginosa* for 10-
226 15 years at the time of sampling. All four individuals had at least one copy of the F508del CFTR
227 mutation, but none were on CFTR modulator therapy. Patients 1, 2, and 4 were seeking outpatient
228 treatment for an acute pulmonary exacerbation at the time of sampling, while Patient 3 was in
229 stable medical condition. These individuals were in the early (%FEV_1 > 70) to intermediate
230 (%FEV_1 ≤ 70, ≥ 40) stages of lung disease, with %FEV_1 scores ranging from 60.30% to 74.92%.
231 The antibiotic regimens for each patient at the time of sampling were as follows: Patient 1 was
232 receiving inhaled tobramycin and oral azithromycin; Patient 2 was receiving inhaled tobramycin
233 and oral trimethoprim/ sulfamethoxazole; Patient 3 was receiving inhaled tobramycin, oral
234 azithromycin, and inhaled aztreonam; and Patient 4 was receiving inhaled tobramycin, oral
235 trimethoprim/ sulfamethoxazole, and oral levofloxacin (**Table 1**).
236
237 ***P. aeruginosa* populations display significant within-patient diversity in antimicrobial**
238 **resistance profiles.** In order to assess diversity in AMR, we selected 75 isolates from a single
239 sputum sample of each of the four individuals for a total of 300 isolates. Using a standard disc

240 diffusion assay, we assessed these 300 isolates for their susceptibilities to six antimicrobials
241 commonly prescribed in CF treatment: amikacin, meropenem, piperacilin-tazobactam,
242 ciprofloxacin, tobramycin, and ceftazidime (**Tables S1-S4**). Zone of inhibition values within a
243 population for a given antibiotic displayed a statistical range (minimum subtracted from the
244 maximum value of a population) between 6 and 25.3 mm, with an average of 12.75 mm. Standard
245 deviations of these values ranged from 1.4 to 8.0 mm, with an average standard deviation of 3.0
246 mm. The majority of isolates presented values well within the range of susceptibility for the tested
247 antibiotics, despite ineffective clearing of infection in the clinic for these patients chronically
248 infected with *P. aeruginosa* (**Fig. 1)**. Only two patients harbored isolates that tested in the range
249 of clinical resistance to any antimicrobial: amikacin, ciprofloxacin, and tobramycin for Patient 1;
250 and ciprofloxacin for Patient 3. Three of the four patients harbored isolates that presented
251 phenotypes spanning across the clinical thresholds for resistant, intermediate, and susceptible
252 for at least one, if not multiple, antibiotics. Principal components analysis of these values show
253 that isolate antimicrobial sensitivity phenotypes cluster by patient (**Fig. 2**).
254
255 **The four patients are chronically infected by a single *P. aeruginosa* strain, populations of**
256 **which display a range of genomic diversity levels.** In order to quantify the level of within-
257 patient genomic diversity for these populations, we sequenced the 75 isolates from each of the
258 four individuals of this cohort. We prepared the sequences of all 300 isolates using *de novo*
259 assembly and annotation. We assembled the genomes in 20 to 444 contigs (mean = 53 contigs;
260 **Table S5**). Genomes in this dataset ranged in size from 5,888,197 to 6,746,489 nucleotides, with
261 5,209 to 5,970 genes (**Table S5**). The median genome sizes of isolates sourced from Patients 1-
262 4, respectively, were 6,222,786, 6,331,110, 6,742,689, and 6,308,671 nucleotides, with 5,523,
263 5,571, 5,964, and 5,567 genes, respectively (**Table S5**). A phylogenetic tree of the core genome
264 alignment revealed that the populations infecting Patients 1, 2, and 4 clustered closely with PAO1,
265 while that of Patient 3 more closely resembled PA14 (**Fig. S1**). Strain typing of the isolates showed
266 that there was a single *P. aeruginosa* strain type in each patient— ST870, ST2999, ST1197, and
267 ST274 for Patients 1-4, respectively (**Table 1**). For the rest of the text, we will simply refer to each
268 population by its respective patient number.
269
270 We assessed the genomic diversity in these populations according to the number of single
271 nucleotide polymorphisms (SNPs) and microindels (insertions and deletions). We found that
272 genomic diversity varied significantly between patients. The total number of unique SNPs
273 discovered across 75 isolates for Patient 1 was 4,592 (maximum number of pairwise SNPs = 611,

274 median number of pairwise SNPs = 199, mean = 208); for Patient 2 was 1,972 (max. = 326,
275 median = 145, mean = 118); for Patient 3 was 1,638 (max. = 150, median = 76, mean = 87); and
276 for Patient 4 was 31 (max. = 8, median = 1, mean = 3) (**Fig. 3; Table 2**). Across the population of
277 Patient 1 we found 498 unique microindels, 307 for Patient 2, 330 for Patient 3, and 14 for Patient
278 4 (**Table 2**).
279
280 **Genomic diversity may not be a consistent predictor of antimicrobial resistance diversity**
281 **in a population.** We next determined whether genomic diversity could serve as a predictor of
282 diversity in AMR phenotypes in our cohort. We hypothesized that genetically diverse populations
283 would also display more diversity in AMR. We chose to quantify genomic diversity in terms of
284 SNPs. We quantified AMR diversity using the number of distinct AMR profiles (i.e., distinct zone
285 of inhibition values) for a given antibiotic within a population. Total SNP count in a population was
286 a strong indicator of AMR diversity for amikacin (R^2 = .90, F(1, 2) = 18.94, p = .049), meropenem
287 (R^2 = .93, F(1, 2) = 25.3, p = .037), and piperacilin-tazobactam (R^2 = .95, F(1, 2) = 39.86, p =
288 .024). However, SNP count was a poor indicator of AMR diversity for ciprofloxacin (R^2 = .12,
289 F(1,2) = .27, p = .65) and ceftazidime (R^2 = .71, F(1,2) = 4.78, p = .16), and was inversely related
290 to AMR diversity for tobramycin (R^2 = .97, F(1,2) = 66.61, p = .015) (**Fig. S2**). We next used the
291 number of distinct CARD resistance genotype profiles within a population (**Fig. 4**) as a proxy for
292 genomic diversity to eliminate bias from SNPs not relevant to AMR and to account for the epistatic
293 or synergistic effect that combinations of various alleles may have. This yielded similar results to
294 the previous analysis (**Table S6**). We then instead used the standard deviation of zone of
295 inhibition values within a population as a proxy for AMR diversity to see if this would improve the
296 strength of the association between genomic diversity and phenotypic diversity for these
297 antimicrobials. We found that the number of distinct CARD profiles within a population was a
298 better predictor of standard deviation for ciprofloxacin (R^2 = .79, F(1,2) = 7.35, p = .11), tobramycin
299 (R^2 = .77, F(1,2) = 6.73, p = .12), and ceftazidime (R^2 = .81, F(1,2) = 8.44, p = .10), though these
300 associations were still not significant (**Fig. S3**).
301
302 ***P. aeruginosa* diversity is primarily driven by *de novo* mutations, especially mutations in**
303 **DNA mismatch repair.** We next wanted to further understand the processes by which *P.*
304 *aeruginosa* diversified in our cohort. We first sought to predict putative recombination events. In
305 Patients 1-4, 527 (11.5%), 19 (<1%), 86 (5.25%), and 0 SNPs were predicted to be in 31, 3, 17,
306 and 0 recombinant regions, respectively. These data show that *de novo* mutation was a much
307 more prominent driver of intra-specific diversity than recombination in our particular cohort. As

308 expected, we found that the infections with the highest SNP diversity harbored strains with DNA
309 MMR mutations. Patients 1 and 2 harbored DNA MMR mutants (hypermutators); however, we
310 found no hypermutators in Patients 3 or 4 (**Fig. 3**). The phylogeny of Patient 1 indicates that a
311 non-synonymous SNP in *mutS* (Ser31Gly) evolved first in the population, after which a frameshift
312 deletion in *mutS* (Ser544fs) piggybacked. In total, *mutS* mutants comprise 61.3% of this
313 population. In Patient 2, a non-synonymous SNP in *mutL* resulting in a pre-mature stop codon
314 (Glu101*) evolved first, found in 41.3% of the population. Two of these *mutL* mutants further
315 independently acquired a single non-synonymous mutation in *mutS* (Phe445Leu, Ala507Thr)
316 (**Fig. 3**).
317
318 In Patient 1, there were two distinct branches of the phylogenetic tree, one with hypermutators
319 and the other composed of normomutators (38.7%) (**Fig. 3**). Interestingly, there was a significant
320 amount of genetic diversity within both the normomutators (mean SNP distance = 156.9 SNPs,
321 median = 91 SNPs) and hypermutators (mean = 174.6 SNPs, median = 197 SNPs). There was a
322 distinct small cluster of normomutator isolates that significantly diverged from the others. Of the
323 hypermutators, these further diverged into those with one DNA MMR mutation (39.1%) and those
324 with two MMR mutations (60.9%). In Patient 2, there was largely a lack of genetic diversity in the
325 normomutators (mean = 0.36 SNPs, median = 0 SNPs), with one clone dominating 48% of the
326 population (**Fig. 3**). The emergence of hypermutators appears to have been responsible for the
327 large majority of all the genetic diversity in this population (mean = 211.2 SNPs, median = 224
328 SNPs). In Patient 3, there were three major lineages, comprising 58.7%, 26.7%, and 14.7% of
329 the total population (mean = 61.9, 55.5, and 65.4 SNPs; median = 62, 61, and 64 SNPs,
330 respectively; **Fig. 3**). In Patient 4, there was one dominant clone encompassing 66.6% of the
331 population, with a small number of SNPs (mean = 4 SNPs, median = 3 SNPs) differentiating the
332 other 33.3% of the population (**Fig. 3**).
333
334 **Hypermutation can drive the evolution of increased susceptibility to antimicrobials, even**
335 **under apparent selective pressure.** As our cohort had two populations with DNA MMR mutants,
336 we used this opportunity to ascertain how hypermutation drives the evolution of AMR. In Patient
337 1, AMR genotypes cluster by DNA MMR genotype. Hypermutators were significantly more
338 resistant to amikacin than normomutators (U = 315.5, p = .00013) (**Fig. 5**), although this difference
339 could not be attributed to any hits in the CARD database. Hypermutators were also significantly
340 more resistant to beta-lactams piperacilin-tazobactam (U = 457.5, p = .023) and ceftazidime (U =
341 428, p = .0095), although there was no significant difference in the resistance profiles of hyper-

342 and normomutators with regards to the beta-lactam meropenem (U = 630, *p* =.69) (**Fig. 5**). Some
343 normomutators in this population acquired a SNP in *ampC* (461 A > G, Asp154Gly) (**Fig. 4**), which
344 was associated with increased sensitivity to piperacilin-tazobactam (U = 320, *p* = .0014) and
345 ceftazidime (U = 342.5, *p* = .0034). Of the isolates with one DNA MMR mutation, some lost *ampC*
346 entirely, also associated with increased susceptibility to ceftazidime (U = 106, *p* = .0019). Of the
347 isolates with both DNA MMR mutations, some had acquired a SNP in *ampC* (1066 G > A,
348 Val356Ile), which appeared to increase their resistance to piperacilin-tazobactam (U = 12, *p* <
349 .00001) and ceftazidime (U = 8, *p* < .00001) (**Fig. 4**).
350
351 Interestingly, hypermutator isolates in this population displayed zone of inhibition values that were
352 on average 10 times larger for ciprofloxacin (U = 218, *p* < .00001) and >13 times larger for
353 tobramycin (U = 379.5, *p* = .0018) than normomutators, indicating increased sensitivity of
354 hypermutators to these antimicrobials (**Fig. 5**). Isolates with both DNA MMR mutations in this
355 population additionally presented ZOI values that were 36 times larger than normomutators for
356 tobramycin (U = 172.5, *p* < .00001) (**Fig. 5**). The altered ciprofloxacin phenotype may be explained
357 in part by SNPs in *gyrA* (248 T > C, Ile83Thr) or *norM* (61 G > A, Ala21Thr) (U = 38.5, *p* < .00001)
358 (**Fig. 4**). However, there were isolates in this population whose phenotypes were not ostensibly
359 explained by either of these genotypes. The increased susceptibility to tobramycin was strongly
360 linked to the aforementioned SNP in *norM* (U = 31.5, *p* < .00001) (**Fig. 4**). We observed apparent
361 evidence of one of these hypermutators reversing this increased susceptibility to tobramycin by
362 acquisition of the aminoglycoside nucleotidyltransferase *ant(2")-Ia* (**Fig. 4**). There was additionally
363 a normomutator isolate with an outlier tobramycin susceptibility phenotype. Interestingly, 12
364 isolates from Patient 1 had improved growth in the presence of tobramycin (determined by visual
365 observation of denser growth in the region surrounding the antibiotic disc in a disc diffusion
366 assay), a phenotype which could not be explained by any hits in the database. All of the
367 normomutator isolates had a truncated *mexF* (**Fig. 4**), although this did not appear to impact any
368 of the tested phenotypes.
369
370 In Patient 2, hypermutators displayed increased sensitivities to meropenem (U = 194, p < .00001),
371 piperacilin-tazobactam (U = 121.5, *p* < .00001), and ciprofloxacin (U = 213.5, *p* < .00001) relative
372 to normomutators (**Fig. 5**). This appeared to be caused in part by a SNP in *mexB* (2257 T > C,
373 Trp753Arg) shared by all hypermutators in this population. However, there were outliers whose
374 phenotype could not be explained by this genotype. Hypermutators were also more susceptible
375 to amikacin (U = 479, *p* = .029) and more resistant to ceftazidime (U = 417.5, *p* = .0045) (**Fig. 5**),

376 although these strains harbored no apparent genes or SNPs associated with these phenotypes
377 in the CARD database. There was no statistically significant difference between the tobramycin
378 susceptibility profiles of hyper- and normomutators in this population (U = 634.5, *p* = .61) (**Fig. 5**).
379 One hypermutator isolate in Patient 2 had an unusual density of truncated pseudogenes, 10 of
380 which are involved in resistance mechanisms and 9 of which specifically play roles in resistance-
381 nodulation-cell division efflux— *mexY*, *mexQ*, *mexN*, *cpxR*, *muxB*, *muxC*, *mexI*, *mexB*, *mexD*,
382 and *cprR* (**Fig. 4**). Although RGI denoted these genes as missing due to truncation, this isolate
383 was equally or more resistant to every antimicrobial tested relative to other DNA MMR mutants in
384 the population, suggesting that many of these genes were still functional.
385
386 In the two normomutator populations, there was significantly decreased resistome diversity. In
387 Patient 3, a SNP in *ampC* (716 T > C, Val239Ala) was associated with increased resistance to
388 ceftazidime (U = 165.5, *p* < .00001) and piperacillin-tazobactam (U = 312.5, *p* = .0045) (**Fig. 4**).
389 Some of the isolates with this SNP additionally were missing *nalC* (**Fig. 4**) and displayed
390 increased susceptibility to meropenem (U = 172.5, *p* = .01778) relative to other isolates. In Patient
391 4, a truncation in *mexY* was strongly linked to variations in sensitivities to amikacin (U = 35, *p* =
392 .0031), piperacillin-tazobactam (U = 22.5, *p* = .0012), ciprofloxacin (U = 0, *p* = .0002), and
393 tobramycin (U = .5, *p* = .00022) (**Fig. 4**). Surprisingly, isolates missing a hit to *aph(3')-IIb* were
394 more resistant to aminoglycosides amikacin (U = 11.5, *p* = .00014) and tobramycin (U = 55, *p* =
395 .00308), and those missing a hit to *ampC* were more resistant to ceftazidime (U = 62, *p* = .0048)
396 (**Fig. 4**). Seeing as these relationships are unexpected, it is likely that there are other genetic
397 variations not cataloged in the CARD database, or epistatic interactions, that are influencing these
398 phenotypes.
399
400 **Protein export/ secretion systems and transcriptional regulators are hotspots for *de novo***
401 **mutations in these populations.** To determine whether these populations were enriched for
402 mutations in genes with roles in resistance, we categorized non-synonymous SNPs and
403 microindels that occurred within coding regions of genes according to the PseudoCAP functional
404 categories and conducted an enrichment analysis. We did not find that AMR genes were enriched
405 for such variants in this cohort (**Fig. S4**). However, we found that protein secretion and export
406 apparatuses and transcriptional regulators were enriched for such mutations (**Fig. S4**).
407 Additionally, two of the four genes impacted by non-synonymous mutations in all four populations
408 in this study were related to protein secretion, *fha1* and *pscP* (**Table S7**). We found that
409 phage/transposon/plasmid genes were less likely to be impacted by such mutations (**Fig. S4**).

410 Non-coding RNAs were also less likely to be impacted by mutations than other functional
411 categories (**Fig. S4**; see **Table S8** for all supporting statistical values), which is unsurprising given
412 that small non-coding RNAs are known to hold important regulatory functions in bacteria [58]. 57
413 genes were impacted by non-synonymous mutations in at least 3 of 4 patients, which included
414 genes with previously described functions in alginate biosynthesis, primary metabolism, antibiotic
415 resistance and efflux, iron uptake, biofilm formation, stress response, amino acid biosynthesis,
416 type IV pili, lipopolysaccharide, quorum sensing, and virulence (**Table S9**). A full list of all SNPs
417 discovered in this dataset can be found in **Tables S10-S13**.
418
419 **Populations display poor evidence for evolutionary trade-offs to explain heterogeneity in**
420 **resistance profiles.** We next wanted to ascertain if there was any evidence of evolutionary trade-
421 offs involving AMR in these populations. Collateral sensitivity is sensitive to genetic background
422 [17, 19, 59, 60] and must be proven robust across a wide range of genetic backgrounds in order
423 to be broadly applicable as a therapeutic strategy [61]. Therefore, we searched for evidence of
424 collateral sensitivity within our populations, and additionally for evidence of trade-offs between
425 AMR and fitness (i.e., growth rate) in a CF sputum-like medium, SCFM [42]. Using the Pearson's
426 correlation coefficient, we found no evidence of collateral sensitivity across any of the six
427 antimicrobials tested for any patient (**Fig. 6**). A principal components analysis conducted for each
428 patient further confirmed this, and showed that cross-resistance and cross-sensitivity patterns
429 differed between patients (**Fig. S5**). We analyzed growth curves for all 300 isolates (**Tables S14-**
430 **S17**) and using a linear mixed model, determined that there was not a significant relationship
431 between resistance and fitness for any of the tested antimicrobials (**Fig. S6; Table S18** for
432 supporting code and statistical values).
433
434 **Discussion**
435 The goal of this project was to better understand how genomic diversification in *P. aeruginosa* CF
436 lung populations drives the evolution of AMR. For this study, we selected four distinct patients
437 with varying levels of *P. aeruginosa* genomic population diversity, ranging from a few dozen to
438 multiple thousands of SNPs within a given population. We found that (i) genomic diversity was
439 not consistently a reliable predictor of AMR diversity for this cohort; (ii) hypermutators in one
440 population evolved increased sensitivity to tobramycin, even when undergoing treatment by
441 tobramycin; and that (iii) there was no evidence for collateral sensitivity or trade-offs between
442 AMR and fitness in these populations.
443

444 Previous studies have reported both on genomic and phenotypic diversity of *P. aeruginosa* in CF
445 airways [6, 34-40]; however, the clinical implications of genomic diversity within these populations
446 on resistance diversity have not been fully assessed. Our results suggest that genomic diversity
447 may not be a reliable predictor of phenotypic diversity for all antibiotics. However, there are a
448 number of limitations to this finding: (i) our sample size for this analysis was small; (ii) we cannot
449 account for diverse genotypes that result in converging phenotypes; and (iii) there are likely many
450 genetic variants that act on AMR that have not been catalogued in CARD. Nonetheless, we
451 highlight that Patient 4 displayed a number of distinct AMR profiles that was, in the case of
452 ciprofloxacin, comparable to that of Patient 1, which had 148x more SNPs and 4x as many distinct
453 CARD genotype profiles within the population. In the case of tobramycin, Patient 4 displayed more
454 distinct AMR profiles and higher zone of inhibition standard deviation values compared to Patients
455 2 and 3, which both had 2x as many distinct CARD genotype profiles and over 53x more
456 population SNPs compared to Patient 4. Ultimately, because of our limited ability at present to
457 predict the phenotypic impact of novel genetic variants or the epistatic interactions of alleles *in*
458 *silico*, it may prove challenging to ascertain the phenotypic heterogeneity of an infection in a
459 parsimonious manner that could be translated to the clinic [41]. In addition to improved *in silico*
460 capabilities, greater understanding of the social interactions that impact how co-infecting microbes
461 with varying resistance levels collectively respond to antibiotic treatment and development of
462 reliable methodology for assessing population-level resistance are also necessary. Considering
463 the impact of polymicrobial interactions has certainly been shown to add an additional layer of
464 complexity in predicting the antimicrobial sensitivity profiles of diverse infections [32, 62], although
465 there is still uncertainty in the degree to which various species of pathogens spatially co-exist and
466 interact in the CF lung. Improved understanding of how these social dynamics influence AMR
467 may be instrumental in future approaches for tackling chronic infections.
468
469 Our data further highlight that even our ability to assess resistance at the isolate-level is
470 inadequate. Though the majority of the isolates selected for this study demonstrated sensitivity to
471 nearly every antibiotic *in vitro*, these testing results likely underestimate resistance levels *in situ*,
472 given that these populations have persisted within the lung for over a decade and that only one
473 population displayed clinical resistance to tobramycin, despite all four individuals in this cohort
474 undergoing treatment with inhaled tobramycin. These findings are in accordance with the wide
475 array of literature that has already called into question the utility of antimicrobial susceptibility
476 testing in the clinic, which falls short in reproducing the hypoxic CF microenvironment and the
477 biofilm mode of growth displayed by *P. aeruginosa* in this biological context, and ultimately fails

478 in predicting patient outcomes [5, 63, 64]. Still, we found it particularly unusual that two of our
479 populations did not display clinical resistance to any of the antimicrobials tested *in vitro*, as prior
480 studies on AMR diversity of *P. aeruginosa* in CF lungs have generally demonstrated high
481 prevalence of *in vitro* resistance within populations [34-38].
482
483 Two limitations of our study are that we were unable to obtain full treatment histories for these
484 patients, and that the pre-selected panel of antimicrobials tested did not include all those that the
485 four patients were undergoing treatment with at the time of sampling (i.e., aztreonam,
486 azithromycin, trimethoprim-sulfamethoxazole, and levofloxacin). Disc diffusion data on these
487 antimicrobials in addition to treatment histories of these patients could potentially illuminate the
488 reasons for treatment failure and explain the presence of strains resistant to amikacin and
489 ciprofloxacin. However, (i) the mechanisms of resistance for levofloxacin and aztreonam closely
490 overlap with those of the other aminoglycoside and beta-lactam antibiotics tested; (ii)
491 trimethoprim-sulfamethoxazole is not prescribed as a treatment for *P. aeruginosa*; and (iii)
492 azithromycin does not display conventional antimicrobial activity against *P. aeruginosa*, but rather,
493 inhibits quorum sensing (therefore, rendering traditional disc diffusion testing of this drug non-
494 viable). Therefore, we believe that our results still broadly provide coverage of the spectrum of
495 relevant antimicrobial sensitivities displayed by these populations. We were additionally
496 concerned to discover strains with increased growth in the presence of tobramycin, as inhaled
497 tobramycin is one of the most commonly prescribed drugs for CF patients with *P. aeruginosa*
498 infection. It may be that tobramycin is being catabolized by these strains to aid in growth, although
499 further investigation is needed to test this hypothesis.
500
501 Combining single-isolate whole genome sequencing and phenotypic characterization approaches
502 further allowed us to understand how the evolution of genotypes and combination of alleles impact
503 AMR within a population. Although we were able to identify a number of candidate genotypes
504 responsible for these phenotypic variations, there were a number of unexplained phenotypic
505 outliers, highlighting the presence of novel genetic signatures of AMR or allelic interactions
506 influencing AMR phenotype. Previous reports have primarily focused on the role that
507 hypermutation plays in evolving increased AMR in clinical *P. aeruginosa* populations [65-71]. We
508 found ample evidence that hypermutation can also lead to increased susceptibility, such as the
509 hypermutator isolates in Patient 1 that were significantly more sensitive to tobramycin, despite
510 this patient undergoing treatment with inhaled tobramycin. This may be a function of antimicrobial
511 treatment regimens exerting uneven selection pressure on the population. Or, it may be that the

512 evolution of genetic resistance for these populations is inconsequential because antimicrobials
513 are failing to penetrate phenotypic barriers, such as biofilms, and other mechanisms of antibiotic
514 tolerance, including persister cells with reduced metabolic activity in the microaerophilic lung [72-
515 78]. Although antimicrobial treatment leads to increased resistance *in vitro* [79-85], the
516 development of resistance or sensitivity *in vivo* may, in some ways, be a result of stochastic
517 processes or other evolutionary drivers if antibiotic treatment regimens are only exerting weak
518 selective pressure.
519
520 It is often assumed that the evolution of AMR involves a fitness cost, although this has
521 predominantly been tested in lab-evolved strains [15, 85-88]. We found no evidence for collateral
522 sensitivity or trade-offs between resistance and fitness in a CF-like medium for these clinical
523 populations. However, in interpreting these results, we must consider that *in vitro* susceptibility
524 and growth testing does not accurately recapitulate the infectious microenvironment of an *in vivo*
525 lung [64]. Therefore, trade-offs between these measures may be present in the lung but not
526 detectable under laboratory conditions. Collateral sensitivity, although shown in evolutionary
527 experiments [15-19], has yet to be demonstrated as widely prevalent in naturally occurring clinical
528 strains. Further work is needed to show that collateral sensitivity is a viable approach for future
529 therapeutic consideration. A recent report found evidence for trade-offs between fitness and multi-
530 drug resistance in clinical *P. aeruginosa* populations [89]. Taken together with our results, we
531 hypothesize that resistance to a single antibiotic may not exert sufficient fitness cost to act as a
532 driving force for trade-offs with growth rate, while resistance to multiple antibiotics perhaps does.
533 Furthermore, this study found stronger evidence for trade-offs in mixed strain infections, whereas
534 all of the individuals in our cohort were infected with a single strain of *P. aeruginosa*. Moreover,
535 as the majority of our strains were technically clinically sensitive to the tested antimicrobials, we
536 may not have had the power to detect trade-offs if they are only elicited at high resistance levels.
537 If resistance does indeed trade-off with fitness, this suggests that slow-growing strains may prove
538 to be the most resistant to treatment. The implication of this for the clinic is concerning, as the
539 slowest growing strains may be more likely to remain undetected during routine susceptibility
540 testing in the clinic, where quick results are favored in order to expedite treatment.
541
542 Conducting deep sampling of clinical *P. aeruginosa* populations has allowed us to illuminate
543 population structure, evolution, and population diversity in CF in a manner that single-isolate
544 sampling or population-level sequencing cannot. These methods suffer in their ability to identify
545 rare variants, accurately resolve population structure, and in the case of pooled deep-sequencing,

link genotype to phenotype for individual isolates. A 2016 study claimed that single-isolate sampling of longitudinal isolates was sufficient to capture the evolutionary pathways of *P. aeruginosa* in CF lung infection; however, the authors conducted metagenome sequencing at a low depth of 10-31x and only sought to determine if SNPs within individual isolates could be re-discovered in the metagenomes, not whether the individual isolates captured the full diversity of the metagenome [90]. However, we believe there is still incredible value in conducting longitudinal analyses. Building upon previous work [91], we propose that conducting deeper sampling of populations over long time scales will help illuminate the full evolutionary dynamics of *P. aeruginosa* populations in the CF lung and lead to insights that will assist in tackling chronic infections.

Acknowledgements

For funding, we thank the Georgia Institute of Technology, the Cystic Fibrosis Foundation for grants (DIGGLE18I0 and DIGGLE20G0) to S.P.D. and a fellowship to S.A. (AZIMI18F0), CF@LANTA for a fellowship to S.A. (3206AXB), the National Institutes of Health for a grant (R01AI153116) to S.P.D and T.R., and the National Science Foundation for a fellowship to J.V. (DGE-2039655). Any opinion, findings, and conclusions or recommendations expressed in this material are those of the authors and do not necessarily reflect the views of the funding agencies. Access to the Cystic Fibrosis Biospecimen Registry at Emory Children's Center for CF and Airways Disease Research was provided through Children's Healthcare of Atlanta and the Emory University Pediatric CF Discovery Core. We thank Arlene Stecenko and Katy Clemmer for assistance in acquiring sputum samples.

Author contributions

All authors contributed to research design; J.V. performed research and analyzed data; all authors contributed to writing the paper.

Figure legends

Figure 1. Violin plot of the antimicrobial susceptibility profiles of all four populations against amikacin, meropenem, piperacillin-tazobactam, ciprofloxacin, tobramycin, and ceftazidime as measured by zone of inhibition in a standard disc diffusion assay shows phenotypic diversity across all populations. Data points are clustered and colored by respective patient, with each individual violin plot representing 75 isolates from a single patient. Black horizontal bars indicate the cut-off values for susceptibility (top bar) and resistance (bottom bar) for each antibiotic as

580 determined by the Clinical and Laboratory Standards Institute (CLSI). Clinical thresholds for
581 resistance to amikacin, meropenem, piperacillin-tazobactam, ciprofloxacin, tobramycin, and
582 ceftazidime are 14, 15, 14, 18, 12, and 14 mm, respectively. Clinical thresholds for sensitivity to
583 these antimicrobials are 17, 19, 21, 25, 15, and 18 mm, respectively.
584
585 **Figure 2.** Principal components analysis plot of antimicrobial sensitivities shows that isolates
586 cluster by patient. 50.5% of the variance in antimicrobial sensitivities is demonstrated by
587 dimension 1, and 32.9% of the variance is demonstrated by dimension 2. Vectors demonstrate to
588 what degree each variable (i.e., antimicrobial) influences the principal components.
589
590 **Figure 3.** Genomic diversity as measured by core genome SNPs varies greatly from one
591 population to another. Populations are presented in order of decreasing genomic diversity: Patient
592 1 (A), Patient 2 (B), Patient 3 (C), and Patient 4 (D). Each matrix represents the pairwise
593 comparison of SNPs across all 75 isolates within a population against each other, and each
594 population is composed of a single strain type. Isolates with one DNA mismatch repair mutation
595 are highlighted in yellow on phylogenies. Isolates with two DNA mismatch repair mutations are
596 highlighted in red.
597
598 **Figure 4.** Visualized resistomes of Patients 1 (A), 2 (B), 3 (C), and 4 (D) as predicted by the
599 Comprehensive Antibiotic Resistance Database Resistance Gene Identifier (CARD RGI)
600 demonstrate decreasing levels of resistome diversity. Yellow indicates a perfect hit to the
601 database, teal indicates a strict hit, and purple indicates no hit (or loose hit in some cases). X-axis
602 of the histogram indicates the number of unique resistome profiles in the population, and y-axis
603 indicates the number of isolates in the population that share a unique resistome profile. An
604 asterisk (*) indicates a gene with resistance conferred by a mutation (i.e. CARD RGI protein
605 variant model).
606
607 **Figure 5.** Comparative antimicrobial susceptibility profiles of hypermutators and normomutators
608 in Patient 1 (A) and Patient 2 (B) as measured by zone of inhibition in a standard disc diffusion
609 assay highlight increased sensitivities and resistance levels by hypermutators. (A) In Patient 1,
610 hypermutators were significantly more resistant to amikacin ($U = 315.5$, $p = .00013$), piperacilin-
611 tazobactam ($U = 457.5$, $p = .023$), and ceftazidime ($U = 428$, $p = .0095$) than normomutators,
612 although there was no significant difference in the resistance profiles of hyper- and
613 normomutators in regards to meropenem ($U = 630$, $p = .69$). Hypermutator isolates in Patient 1

614 displayed zone of inhibition (ZOI) values that were on average 10 times larger for ciprofloxacin (U
615 = 218, p < .00001) and >13 times larger for tobramycin (U = 379.5, p = .0018) than normomutators,
616 and isolates with both DNA MMR mutations in this population additionally presented ZOI values
617 that were 36 times larger than normomutators for tobramycin (U = 172.5, p < .00001), indicating
618 increased sensitivity displayed by hypermutators. (B) In Patient 2, hypermutators displayed
619 increased susceptibility to amikacin (U = 479, p = .029), meropenem (U = 194, p < .00001),
620 piperacilin-tazobactam (U = 121.5, p < .00001), and ciprofloxacin (U = 213.5, p < .00001) relative
621 to normomutators. Hypermutators in Patient 2 were more resistant to ceftazidime (U = 417.5, p =
622 .0045). There was no statistically significant difference between the tobramycin susceptibility
623 profiles of hyper- and normomutators in this population (U = 634.5, p = .61). (*) indicates p ≤ .05,
624 (**) indicates p ≤ .01, (***) indicates p ≤ .001, and (****) indicates p < .0001 in a Mann-Whitney U
625 test. Clinical thresholds for resistance to amikacin, meropenem, piperacillin-tazobactam,
626 ciprofloxacin, tobramycin, and ceftazidime as determined by the CLSI are 14, 15, 14, 18, 12, and
627 14 mm, respectively. Clinical thresholds for sensitivity to these antimicrobials are 17, 19, 21, 25,
628 15, and 18 mm, respectively.
629
630 **Figure 6.** Lack of statistically significant negative correlations between any two antimicrobial
631 susceptibility profiles in a Pearson's correlation provides no evidence for collateral sensitivity
632 trade-offs. Pearson's correlation coefficient (upper right quadrant), scatterplots (lower left
633 quadrant), and density plots (diagonal) for pairwise comparisons of susceptibility profiles across
634 all six tested antimicrobials: amikacin (AK), meropenem (MEM), piperacillin-tazobactam (TZP),
635 ciprofloxacin (CIP), tobramycin (TOB), and ceftazidime (CAZ).
636
637 **Table 1.** Metadata on the four patients in our cohort: sex, cystic fibrosis transmembrane
638 conductance regulator (CFTR) mutation status, length of *P. aeruginosa* infection, clinical status,
639 forced expiratory volume (% FEV1), modulator therapy, antibiotic treatment at time of sampling,
640 and dominant infection strain type.
641
642 **Table 2.** Genetic variations in each population: single nucleotide polymorphisms (SNPs), multiple
643 nucleotide polymorphisms (MNPs), and insertions and deletions (indels).
644
645 **Supplemental figure legends**
646 **Supplemental Figure 1.** Phylogeny of Patients 1-4 with PAO1 and PA14. Patients 1, 2, and 4
647 cluster with PAO1, while Patient 3 clusters with PA14.

648

649 **Supplemental Figure 2.** Linear regression analysis demonstrates that total SNP count in a
650 population was a strong indicator of AMR diversity for amikacin (R^2 = .90, F(1, 2) = 18.94, *p* =
651 .049), meropenem (R^2 = .93, F(1, 2) = 25.3, *p* = .037), and piperacilin-tazobactam (R^2 = .95, F(1,
652 2) = 39.86, *p* = .024), but a poor indicator of AMR diversity for ciprofloxacin (R^2 = .12, F(1,2) =
653 .27, *p* = .65) and ceftazidime (R^2 = .71, F(1,2) = 4.78, *p* = .16), and was inversely related to AMR
654 diversity for tobramycin (R^2 = .97, F(1,2) = 66.61, *p* = .015)

655

656 **Supplemental Figure 3.** Linear regression analysis shows that the number of distinct CARD
657 profiles within a population is an improved predictor of population standard deviation for
658 ciprofloxacin (R^2 = .79, F(1,2) = 7.35, *p* = .11), tobramycin (R^2 = .77, F(1,2) = 6.73, *p* = .12), and
659 ceftazidime (R^2 = .81, F(1,2) = 8.44, *p* = .10) over total population SNP count.

660

661 **Supplemental Figure 4.** Enrichment analysis of the frequency of functional categories in which
662 non-synonymous SNPs and microindels are found in each of the four populations relative to the
663 proportions of these functional categories in the PAO1 genome shows that protein secretion/
664 export apparatuses and transcriptional regulators are enriched for such variants, while phage/
665 transposon/ plasmid and non-coding RNA are less likely to be impacted by such variants. Donut
666 plot of the relative frequencies of genes categorized within each of the 27 different PseudoCAP
667 functional categories in the PAO1 genome (A). Donut plots of the relative frequencies of non-
668 synonymous SNPs and indels located in each of the 27 different PseudoCAP functional
669 categories in Patient 1 (B), 2 (C), 3 (D), and 4 (E). Protein secretion/ export apparatuses and
670 transcriptional regulators are denoted with green asterisks on donut plots where applicable, while
671 phage/ transposon/ plasmid and non-coding RNA are denoted with red asterisks.

672

673 **Supplemental Figure 5.** Principal components analysis vectors display no evidence of collateral
674 sensitivity across any of the six antimicrobials tested for any patient, and further demonstrate that
675 cross-resistance and cross-sensitivity patterns differ across patients.

676

677 **Supplemental Figure 6.** Scatterplots of zone of inhibition (ZOI) versus growth rate (r) in SCFM
678 for all six tested antibiotics: amikacin (AK), meropenem (MEM), piperacillin-tazobactam (TZP),
679 ciprofloxacin (CIP), tobramycin (TOB), and ceftazidime (CAZ). Results of linear mixed model
680 (Table S18), with growth rate in SCFM as a fixed effect and patient as a random effect,

681 demonstrate that there is no significant effect of growth rate on resistance, and therefore, no
682 evidence for trade-offs between growth rate and resistance in these four populations.
683
684 **Supplemental Table 1.** Antimicrobial susceptibility testing measurements for Patient 1 as
685 measured by zone of inhibition (ZOI) in a standard disc diffusion assay for amikacin (AK),
686 meropenem (MEM), piperacilin-tazobactam (TZP), ciprofloxacin (CIP), tobramycin (TOB), and
687 ceftazidime (CAZ). Data in the left columns represent raw measurements of zone of inhibition
688 radii (mm units). Data in the right columns represent calculated zone of inhibition values as
689 diameters (mm units).
690
691 **Supplemental Table 2.** Antimicrobial susceptibility testing measurements for Patient 2 as
692 measured by zone of inhibition (ZOI) in a standard disc diffusion assay for amikacin (AK),
693 meropenem (MEM), piperacilin-tazobactam (TZP), ciprofloxacin (CIP), tobramycin (TOB), and
694 ceftazidime (CAZ). Data in the left columns represent raw measurements of zone of inhibition
695 radii (mm units). Data in the right columns represent calculated zone of inhibition values as
696 diameters (mm units).
697
698 **Supplemental Table 3.** Antimicrobial susceptibility testing measurements for Patient 3 as
699 measured by zone of inhibition (ZOI) in a standard disc diffusion assay for amikacin (AK),
700 meropenem (MEM), piperacilin-tazobactam (TZP), ciprofloxacin (CIP), tobramycin (TOB), and
701 ceftazidime (CAZ). Data in the left columns represent raw measurements of zone of inhibition
702 radii (mm units). Data in the right columns represent calculated zone of inhibition values as
703 diameters (mm units).
704
705 **Supplemental Table 4.** Antimicrobial susceptibility testing measurements for Patient 4 as
706 measured by zone of inhibition (ZOI) in a standard disc diffusion assay for amikacin (AK),
707 meropenem (MEM), piperacilin-tazobactam (TZP), ciprofloxacin (CIP), tobramycin (TOB), and
708 ceftazidime (CAZ). Data in the left columns represent raw measurements of zone of inhibition
709 radii (mm units). Data in the right columns represent calculated zone of inhibition values as
710 diameters (mm units).
711
712 **Supplemental Table 5.** Genome size, average sequencing coverage, and number of contigs of
713 each assembly.
714

715 **Supplemental Table 6.** Supporting statistical values of the linear regression analysis of distinct
716 CARD resistance genotype profiles within a population as a proxy for genomic diversity as
717 measured by total SNPs in each population.
718
719 **Supplemental Table 7.** Genes that were impacted by non-synonymous mutations in at least one
720 isolate in all four populations.
721
722 **Supplemental Table 8.** Full details of the chi-squared goodness of fit and Monte Carlo simulation
723 exact multinomial tests, with all associated chi-squared and p-values.
724
725 **Supplemental Table 9.** Genes that were impacted by non-synonymous mutations in at least one
726 isolate in three out of four populations.
727
728 **Supplemental Table 10.** All annotated genetic variants discovered in Patient 1.
729
730 **Supplemental Table 11.** All annotated genetic variants discovered in Patient 2.
731
732 **Supplemental Table 12.** All annotated genetic variants discovered in Patient 3.
733
734 **Supplemental Table 13.** All annotated genetic variants discovered in Patient 4.
735
736 **Supplemental Table 14.** Raw OD_{600} reads for growth in SCFM used to create growth curves and
737 analyze growth rate (r) for Patient 1. Time is given in hours, and all isolates were tested in
738 biological triplicates.
739
740 **Supplemental Table 15.** Raw OD_{600} reads for growth in SCFM used to create growth curves and
741 analyze growth rate (r) for Patient 2. Time is given in hours, and all isolates were tested in
742 biological triplicates.
743
744 **Supplemental Table 16.** Raw OD_{600} reads for growth in SCFM used to create growth curves and
745 analyze growth rate (r) for Patient 3. Time is given in hours, and all isolates were tested in
746 biological triplicates.
747

748 **Supplemental Table 17.** Raw OD_{600} reads for growth in SCFM used to create growth curves and
749 analyze growth rate (r) for Patient 4. Time is given in hours, and all isolates were tested in
750 biological triplicates.
751
752 **Supplemental Table 18.** Supporting brms R code and statistical values for the linear mixed model
753 run to assess the relationship between growth rate (r) and antimicrobial resistance. Results of the
754 model, with growth rate in SCFM as a fixed effect and patient as a random effect, show that the
755 95% confidence interval of the fixed effect of growth rate spans 0 for all six antimicrobials.
756 Therefore, the null hypothesis that the fixed effect of growth on antimicrobial susceptibility is 0
757 cannot be rejected, providing no evidence for trade-offs or any significant relationship between
758 resistance and growth rate across all four populations.
759
760
761

762 **Literature**
763
764 1. Davies, J.C., *Pseudomonas aeruginosa* in cystic fibrosis: pathogenesis and persistence.
765 Paediatr Respir Rev, 2002. **3**(2): p. 128-34.
766 2. Foundation, C.F., Cystic Fibrosis Foundation Patient Registry 2020 Annual Data Report.
767 2021.
768 3. Jackson, L. and V. Waters, Factors influencing the acquisition and eradication of early
769 *Pseudomonas aeruginosa* infection in cystic fibrosis. J Cyst Fibros, 2021. **20**(1): p. 8-16.
770 4. Hoiby, N., O. Ciofu, and T. Bjarnsholt, *Pseudomonas aeruginosa* biofilms in cystic
771 fibrosis. Future Microbiol, 2010. **5**(11): p. 1663-74.
772 5. Van den Bossche, S., et al., The cystic fibrosis lung microenvironment alters antibiotic
773 activity: causes and effects. Eur Respir Rev, 2021. **30**(161).
774 6. Jorth, P., et al., Regional Isolation Drives Bacterial Diversification within Cystic Fibrosis
775 Lungs. Cell Host Microbe, 2015. **18**(3): p. 307-19.
776 7. Clark, S.T., D.S. Guttman, and D.M. Hwang, Diversification of *Pseudomonas aeruginosa*
777 within the cystic fibrosis lung and its effects on antibiotic resistance. FEMS Microbiol Lett,
778 2018. **365**(6).
779 8. Bartell, J.A., et al., Omics-based tracking of *Pseudomonas aeruginosa* persistence in
780 "eradicated" cystic fibrosis patients. Eur Respir J, 2021. **57**(4).
781 9. Camus, L., F. Vandenesch, and K. Moreau, From genotype to phenotype: adaptations
782 of *Pseudomonas aeruginosa* to the cystic fibrosis environment. Microb Genom, 2021. **7**(3).
783 10. Mehta, H.H., et al., The Essential Role of Hypermutation in Rapid Adaptation to
784 Antibiotic Stress. Antimicrob Agents Chemother, 2019. **63**(7).
785 11. Lujan, A.M., et al., Polymicrobial infections can select against *Pseudomonas aeruginosa*
786 mutators because of quorum-sensing trade-offs. Nat Ecol Evol, 2022. **6**(7): p. 979-988.
787 12. Armbruster, C.R., et al., Heterogeneity in surface sensing suggests a division of labor in
788 *Pseudomonas aeruginosa* populations. Elife, 2019. **8**.
789 13. Porter, S.S. and K.J. Rice, Trade-offs, spatial heterogeneity, and the maintenance of
790 microbial diversity. Evolution, 2013. **67**(2): p. 599-608.
791 14. Ferenci, T., Trade-off Mechanisms Shaping the Diversity of Bacteria. Trends Microbiol,
792 2016. **24**(3): p. 209-223.
793 15. Barbosa, C., et al., Evolutionary stability of collateral sensitivity to antibiotics in the
794 model pathogen *Pseudomonas aeruginosa*. Elife, 2019. **8**.
795 16. Hernando-Amado, S., F. Sanz-Garcia, and J.L. Martinez, Rapid and robust evolution of
796 collateral sensitivity in *Pseudomonas aeruginosa* antibiotic-resistant mutants. Sci Adv, 2020.
797 **6**(32): p. eaba5493.
798 17. Hernando-Amado, S., et al., Mutational background influences *Pseudomonas*
799 *aeruginosa* ciprofloxacin resistance evolution but preserves collateral sensitivity robustness.
800 Proc Natl Acad Sci U S A, 2022. **119**(15): p. e2109370119.
801 18. Laborda, P., J.L. Martinez, and S. Hernando-Amado, Convergent phenotypic evolution
802 towards fosfomycin collateral sensitivity of *Pseudomonas aeruginosa* antibiotic-resistant
803 mutants. Microb Biotechnol, 2022. **15**(2): p. 613-629.
804 19. Hernando-Amado, S., et al., Rapid Phenotypic Convergence towards Collateral
805 Sensitivity in Clinical Isolates of *Pseudomonas aeruginosa* Presenting Different Genomic
806 Backgrounds. Microbiol Spectr, 2023. **11**(1): p. e0227622.
807 20. Cramer, N., et al., Microevolution of the major common *Pseudomonas aeruginosa*
808 clones C and PA14 in cystic fibrosis lungs. Environ Microbiol, 2011. **13**(7): p. 1690-704.

809 21. Marvig, R.L., et al., Genome analysis of a transmissible lineage of pseudomonas
810 aeruginosa reveals pathoadaptive mutations and distinct evolutionary paths of hypermutators.
811 PLoS Genet, 2013. **9**(9): p. e1003741.
812 22. Feliziani, S., et al., Coexistence and within-host evolution of diversified lineages of
813 hypermutable *Pseudomonas aeruginosa* in long-term cystic fibrosis infections. PLoS Genet,
814 2014. **10**(10): p. e1004651.
815 23. Markussen, T., et al., Environmental heterogeneity drives within-host diversification and
816 evolution of *Pseudomonas aeruginosa*. mBio, 2014. **5**(5): p. e01592-14.
817 24. Marvig, R.L., et al., Within-host microevolution of *Pseudomonas aeruginosa* in Italian
818 cystic fibrosis patients. BMC Microbiol, 2015. **15**: p. 218.
819 25. Marvig, R.L., et al., Convergent evolution and adaptation of *Pseudomonas aeruginosa*
820 within patients with cystic fibrosis. Nat Genet, 2015. **47**(1): p. 57-64.
821 26. Bianconi, I., et al., Persistence and Microevolution of *Pseudomonas aeruginosa* in the
822 Cystic Fibrosis Lung: A Single-Patient Longitudinal Genomic Study. Front Microbiol, 2018. **9**: p.
823 3242.
824 27. Klockgether, J., et al., Long-Term Microevolution of *Pseudomonas aeruginosa* Differs
825 between Mildly and Severely Affected Cystic Fibrosis Lungs. Am J Respir Cell Mol Biol, 2018.
826 **59**(2): p. 246-256.
827 28. Gabrielaite, M., et al., Gene Loss and Acquisition in Lineages of *Pseudomonas*
828 *aeruginosa* Evolving in Cystic Fibrosis Patient Airways. mBio, 2020. **11**(5).
829 29. Datar, R., et al., Phenotypic and Genomic Variability of Serial Peri-Lung Transplantation
830 *Pseudomonas aeruginosa* Isolates From Cystic Fibrosis Patients. Front Microbiol, 2021. **12**: p.
831 604555.
832 30. Wardell, S.J.T., et al., Genome evolution drives transcriptomic and phenotypic
833 adaptation in *Pseudomonas aeruginosa* during 20 years of infection. Microb Genom, 2021.
834 **7**(11).
835 31. Andersson, D.I., H. Nicoloff, and K. Hjort, Mechanisms and clinical relevance of
836 bacterial heteroresistance. Nat Rev Microbiol, 2019. **17**(8): p. 479-496.
837 32. Reece, E., P.H.A. Bettio, and J. Renwick, Polymicrobial Interactions in the Cystic
838 Fibrosis Airway Microbiome Impact the Antimicrobial Susceptibility of *Pseudomonas*
839 *aeruginosa.* Antibiotics (Basel), 2021. **10**(7).
840 33. Galdino, A.C.M., et al., *Polymicrobial Biofilms in Cystic Fibrosis Lung Infections: Effects*
841 *on Antimicrobial Susceptibility*, in *Multispecies Biofilms: Technologically Advanced Methods to*
842 *Study Microbial Communities*, K.S. Kaushik and S.E. Darch, Editors. 2023, Springer
843 International Publishing: Cham. p. 231-267.
844 34. Mowat, E., et al., *Pseudomonas aeruginosa* population diversity and turnover in cystic
845 fibrosis chronic infections. Am J Respir Crit Care Med, 2011. **183**(12): p. 1674-9.
846 35. Ashish, A., et al., Extensive diversification is a common feature of *Pseudomonas*
847 *aeruginosa* populations during respiratory infections in cystic fibrosis. J Cyst Fibros, 2013.
848 **12**(6): p. 790-3.
849 36. Workentine, M.L., et al., Phenotypic heterogeneity of *Pseudomonas aeruginosa*
850 populations in a cystic fibrosis patient. PLoS One, 2013. **8**(4): p. e60225.
851 37. Clark, S.T., et al., Phenotypic diversity within a *Pseudomonas aeruginosa* population
852 infecting an adult with cystic fibrosis. Sci Rep, 2015. **5**: p. 10932.
853 38. Darch, S.E., et al., Recombination is a key driver of genomic and phenotypic diversity in
854 a *Pseudomonas aeruginosa* population during cystic fibrosis infection. Sci Rep, 2015. **5**: p.
855 7649.

856 39. Williams, D., et al., Divergent, coexisting *Pseudomonas aeruginosa* lineages in chronic
857 cystic fibrosis lung infections. Am J Respir Crit Care Med, 2015. **191**(7): p. 775-85.
858 40. Williams, D., et al., Transmission and lineage displacement drive rapid population
859 genomic flux in cystic fibrosis airway infections of a *Pseudomonas aeruginosa* epidemic strain.
860 Microb Genom, 2018. **4**(3).
861 41. Su, M., S.W. Satola, and T.D. Read, Genome-Based Prediction of Bacterial Antibiotic
862 Resistance. J Clin Microbiol, 2019. **57**(3).
863 42. Palmer, K.L., L.M. Aye, and M. Whiteley, Nutritional cues control *Pseudomonas*
864 *aeruginosa* multicellular behavior in cystic fibrosis sputum. J Bacteriol, 2007. **189**(22): p. 8079-
865 87.
866 43. Petit, R.A., 3rd and T.D. Read, Bactopia: a Flexible Pipeline for Complete Analysis of
867 Bacterial Genomes. mSystems, 2020. **5**(4).
868 44. Jolley, K.A., J.E. Bray, and M.C.J. Maiden, Open-access bacterial population genomics:
869 BIGSdb software, the PubMLST.org website and their applications. Wellcome Open Res, 2018.
870 **3**: p. 124.
871 45. Wick, R.R., et al., Unicycler: Resolving bacterial genome assemblies from short and
872 long sequencing reads. PLoS Comput Biol, 2017. **13**(6): p. e1005595.
873 46. Research, O.N.T., *Medaka*. 2018, Oxford Nanopore Technologies.
874 47. Wick, R.R. and K.E. Holt, Polypolish: Short-read polishing of long-read bacterial
875 genome assemblies. PLoS Comput Biol, 2022. **18**(1): p. e1009802.
876 48. Walker, B.J., et al., Pilon: an integrated tool for comprehensive microbial variant
877 detection and genome assembly improvement. PLoS One, 2014. **9**(11): p. e112963.
878 49. Seemann, T., *Snippy*. 2020.
879 50. Seemann, T., Prokka: rapid prokaryotic genome annotation. Bioinformatics, 2014.
880 **30**(14): p. 2068-9.
881 51. Otto, T.D., et al., RATT: Rapid Annotation Transfer Tool. Nucleic Acids Res, 2011. **39**(9):
882 p. e57.
883 52. Oliver, A., et al., High frequency of hypermutable *Pseudomonas aeruginosa* in cystic
884 fibrosis lung infection. Science, 2000. **288**(5469): p. 1251-4.
885 53. Alcock, B.P., et al., CARD 2023: expanded curation, support for machine learning, and
886 resistome prediction at the Comprehensive Antibiotic Resistance Database. Nucleic Acids Res,
887 2023. **51**(D1): p. D690-D699.
888 54. Engels, B., *XNomial*. 2015.
889 55. Croucher, N.J., et al., Rapid phylogenetic analysis of large samples of recombinant
890 bacterial whole genome sequences using Gubbins. Nucleic Acids Res, 2015. **43**(3): p. e15.
891 56. Sprouffske, K. and A. Wagner, Growthcurver: an R package for obtaining interpretable
892 metrics from microbial growth curves. BMC Bioinformatics, 2016. **17**: p. 172.
893 57. Bürkner, P., brms: An R Package for Bayesian Multilevel Models using Stan. Journal of
894 Statistical Software, 2017. **80**(1): p. 1-28.
895 58. Toledo-Arana, A., F. Repoila, and P. Cossart, *Small noncoding RNAs controlling*
896 *pathogenesis.* Curr Opin Microbiol, 2007. **10**(2): p. 182-8.
897 59. Hernando-Amado, S., et al., Rapid Decline of Ceftazidime Resistance in Antibiotic-Free
898 and Sublethal Environments Is Contingent on Genetic Background. Mol Biol Evol, 2022. **39**(3).
899 60. Genova, R., et al., Collateral Sensitivity to Fosfomycin of Tobramycin-Resistant Mutants
900 of Pseudomonas aeruginosa Is Contingent on Bacterial Genomic Background. Int J Mol Sci,
901 2023. **24**(8).
902 61. Roemhild, R. and D.I. Andersson, Mechanisms and therapeutic potential of collateral
903 sensitivity to antibiotics. PLoS Pathog, 2021. **17**(1): p. e1009172.

904 62. Jean-Pierre, F., et al., Community composition shapes microbial-specific phenotypes in
905 a cystic fibrosis polymicrobial model system. Elife, 2023. **12**.
906 63. Somayaji, R., et al., Antimicrobial susceptibility testing (AST) and associated clinical
907 outcomes in individuals with cystic fibrosis: A systematic review. J Cyst Fibros, 2019. **18**(2): p.
908 236-243.
909 64. Bjarnsholt, T., et al., The importance of understanding the infectious microenvironment.
910 Lancet Infect Dis, 2022. **22**(3): p. e88-e92.
911 65. Macia, M.D., et al., Hypermutation is a key factor in development of multiple-
912 antimicrobial resistance in *Pseudomonas aeruginosa* strains causing chronic lung infections.
913 Antimicrob Agents Chemother, 2005. **49**(8): p. 3382-6.
914 66. Cabot, G., et al., Evolution of *Pseudomonas aeruginosa* Antimicrobial Resistance and
915 Fitness under Low and High Mutation Rates. Antimicrob Agents Chemother, 2016. **60**(3): p.
916 1767-78.
917 67. Khil, P.P., et al., Dynamic Emergence of Mismatch Repair Deficiency Facilitates Rapid
918 Evolution of Ceftazidime-Avibactam Resistance in *Pseudomonas aeruginosa* Acute Infection.
919 mBio, 2019. **10**(5).
920 68. Rees, V.E., et al., Characterization of Hypermutator *Pseudomonas aeruginosa* Isolates
921 from Patients with Cystic Fibrosis in Australia. Antimicrob Agents Chemother, 2019. **63**(4).
922 69. Colque, C.A., et al., Hypermutator Pseudomonas aeruginosa Exploits Multiple Genetic
923 Pathways To Develop Multidrug Resistance during Long-Term Infections in the Airways of
924 Cystic Fibrosis Patients. Antimicrob Agents Chemother, 2020. **64**(5).
925 70. Colque, C.A., et al., Longitudinal Evolution of the Pseudomonas-Derived
926 Cephalosporinase (PDC) Structure and Activity in a Cystic Fibrosis Patient Treated with beta-
927 Lactams. mBio, 2022. **13**(5): p. e0166322.
928 71. Dulanto Chiang, A., et al., Hypermutator strains of *Pseudomonas aeruginosa* reveal
929 novel pathways of resistance to combinations of cephalosporin antibiotics and beta-lactamase
930 inhibitors. PLoS Biol, 2022. **20**(11): p. e3001878.
931 72. Moriarty, T.F., et al., Sputum antibiotic concentrations: implications for treatment of
932 cystic fibrosis lung infection. Pediatr Pulmonol, 2007. **42**(11): p. 1008-17.
933 73. Ciofu, O., et al., Antimicrobial resistance, respiratory tract infections and role of biofilms
934 in lung infections in cystic fibrosis patients. Adv Drug Deliv Rev, 2015. **85**: p. 7-23.
935 74. Sonderholm, M., et al., The Consequences of Being in an Infectious Biofilm:
936 Microenvironmental Conditions Governing Antibiotic Tolerance. Int J Mol Sci, 2017. **18**(12).
937 75. Crabbe, A., et al., Antimicrobial Tolerance and Metabolic Adaptations in Microbial
938 Biofilms. Trends Microbiol, 2019. **27**(10): p. 850-863.
939 76. Martin, I., V. Waters, and H. Grasemann, Approaches to Targeting Bacterial Biofilms in
940 Cystic Fibrosis Airways. Int J Mol Sci, 2021. **22**(4).
941 77. Santi, I., et al., Evolution of Antibiotic Tolerance Shapes Resistance Development in
942 Chronic Pseudomonas aeruginosa Infections. mBio, 2021. **12**(1).
943 78. Witzany, C., R.R. Regoes, and C. Igler, Assessing the relative importance of bacterial
944 resistance, persistence and hyper-mutation for antibiotic treatment failure. Proc Biol Sci, 2022.
945 **289**(1986): p. 20221300.
946 79. Wong, A., N. Rodrigue, and R. Kassen, Genomics of adaptation during experimental
947 evolution of the opportunistic pathogen *Pseudomonas aeruginosa*. PLoS Genet, 2012. **8**(9): p.
948 e1002928.
949 80. Jorgensen, K.M., et al., Sublethal ciprofloxacin treatment leads to rapid development of
950 high-level ciprofloxacin resistance during long-term experimental evolution of *Pseudomonas*
951 *aeruginosa*. Antimicrob Agents Chemother, 2013. **57**(9): p. 4215-21.

952 81. Jorth, P., et al., Evolved Aztreonam Resistance Is Multifactorial and Can Produce
953 Hypervirulence in *Pseudomonas aeruginosa*. mBio, 2017. **8**(5).
954 82. Ahmed, M.N., et al., Evolution of Antibiotic Resistance in Biofilm and Planktonic
955 *Pseudomonas aeruginosa* Populations Exposed to Subinhibitory Levels of Ciprofloxacin.
956 Antimicrob Agents Chemother, 2018. **62**(8).
957 83. Sanz-Garcia, F., S. Hernando-Amado, and J.L. Martinez, Mutation-Driven Evolution of
958 *Pseudomonas aeruginosa* in the Presence of either Ceftazidime or Ceftazidime-Avibactam.
959 Antimicrob Agents Chemother, 2018. **62**(10).
960 84. Wardell, S.J.T., et al., A large-scale whole-genome comparison shows that
961 experimental evolution in response to antibiotics predicts changes in naturally evolved clinical
962 *Pseudomonas aeruginosa*. Antimicrob Agents Chemother, 2019. **63**(12).
963 85. Ahmed, M.N., et al., The evolutionary trajectories of *Pseudomonas aeruginosa* in biofilm
964 and planktonic growth modes exposed to ciprofloxacin: beyond selection of antibiotic
965 resistance. NPJ Biofilms Microbiomes, 2020. **6**(1): p. 28.
966 86. Hernando-Amado, S., et al., Fitness costs associated with the acquisition of antibiotic
967 resistance. Essays Biochem, 2017. **61**(1): p. 37-48.
968 87. Laborda, P., J.L. Martinez, and S. Hernando-Amado, Evolution of Habitat-Dependent
969 Antibiotic Resistance in *Pseudomonas aeruginosa*. Microbiol Spectr, 2022. **10**(4): p. e0024722.
970 88. Jorth, P., et al., *Evolved bacterial siderophore-mediated antibiotic cross-protection.*
971 Preprint available at https://doi.org/10.21203/rs.3.rs-2644953/v1, 2023.
972 89. Diaz Caballero, J., et al., Mixed strain pathogen populations accelerate the evolution of
973 antibiotic resistance in patients. Nat Commun, 2023. **14**(1): p. 4083.
974 90. Sommer, L.M., et al., Is genotyping of single isolates sufficient for population structure
975 analysis of *Pseudomonas aeruginosa* in cystic fibrosis airways? BMC Genomics, 2016. **17**: p.
976 589.
977 91. Diaz Caballero, J., et al., Selective Sweeps and Parallel Pathoadaptation Drive
978 *Pseudomonas aeruginosa* Evolution in the Cystic Fibrosis Lung. mBio, 2015. **6**(5): p. e00981-
979 15.

Fig 1

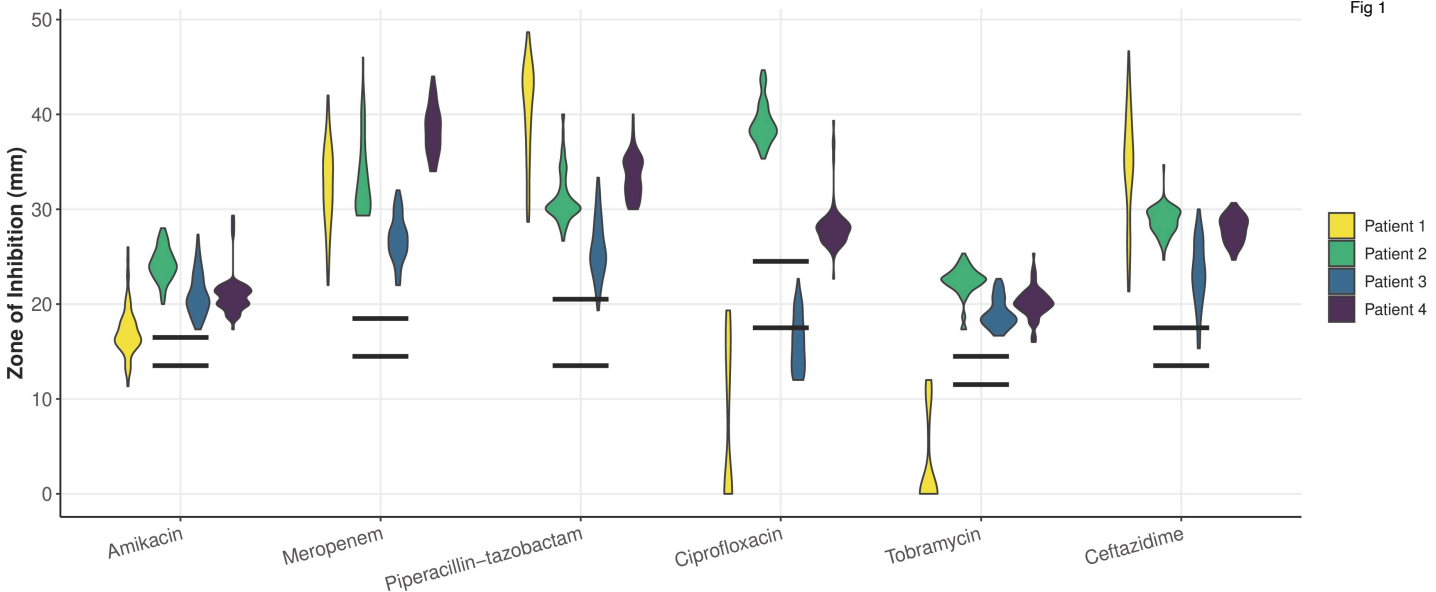
Zone of Inhibition (mm)
50
40
30
20
10
0
Amikacin
Meropenem
Piperacillin–tazobactam
Ciprofloxacin
Tobramycin
Ceftazidime
Patient 1
Patient 2
Patient 3
Patient 4

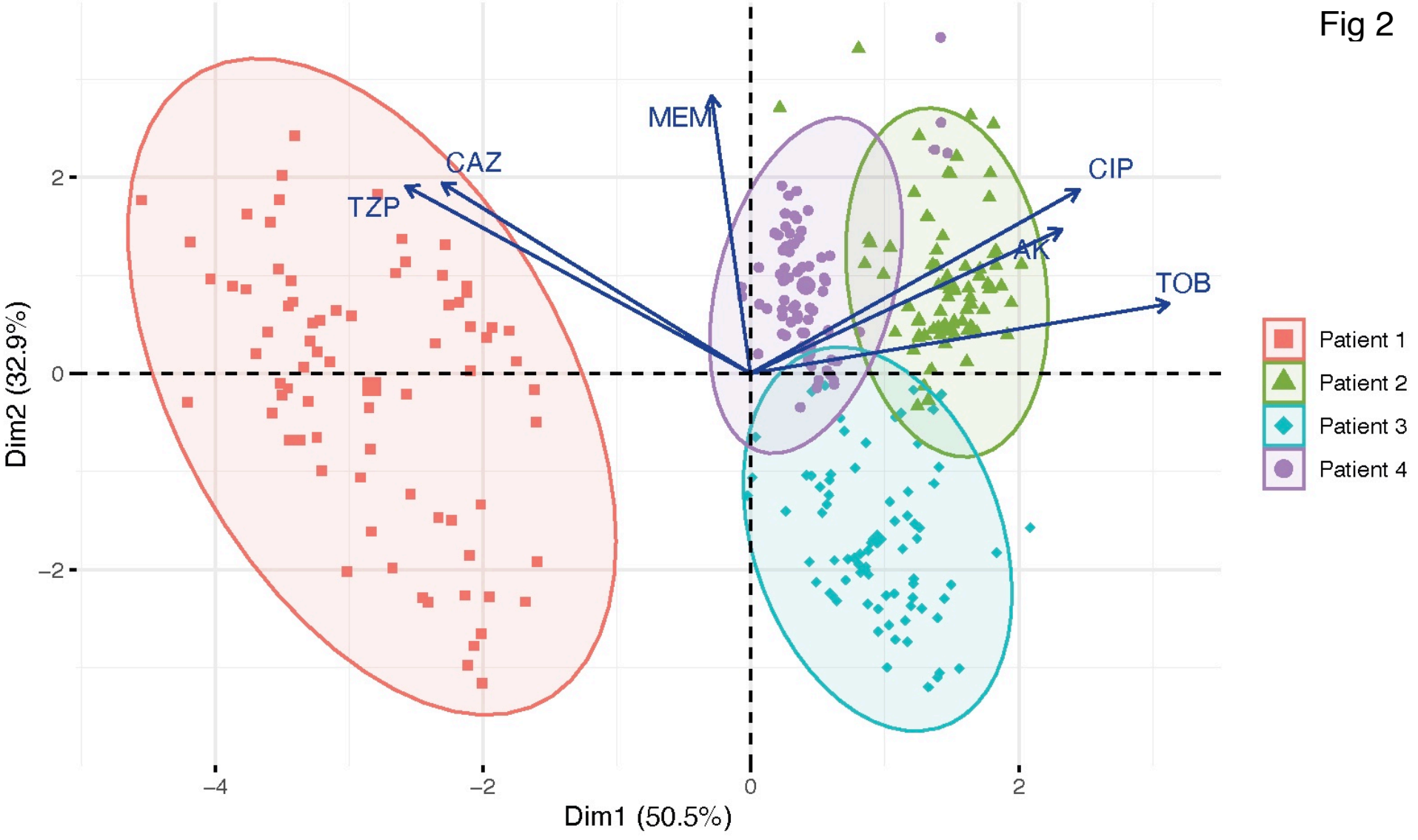
Fig 2
MEM
CAZ
TZP
CIP
AK
TOB
Patient 1
Patient 2
Patient 3
Patient 4
Dim2 (32.9%)
Dim1 (50.5%)
2
0
−2
−4
−2
0
2

Fig 3

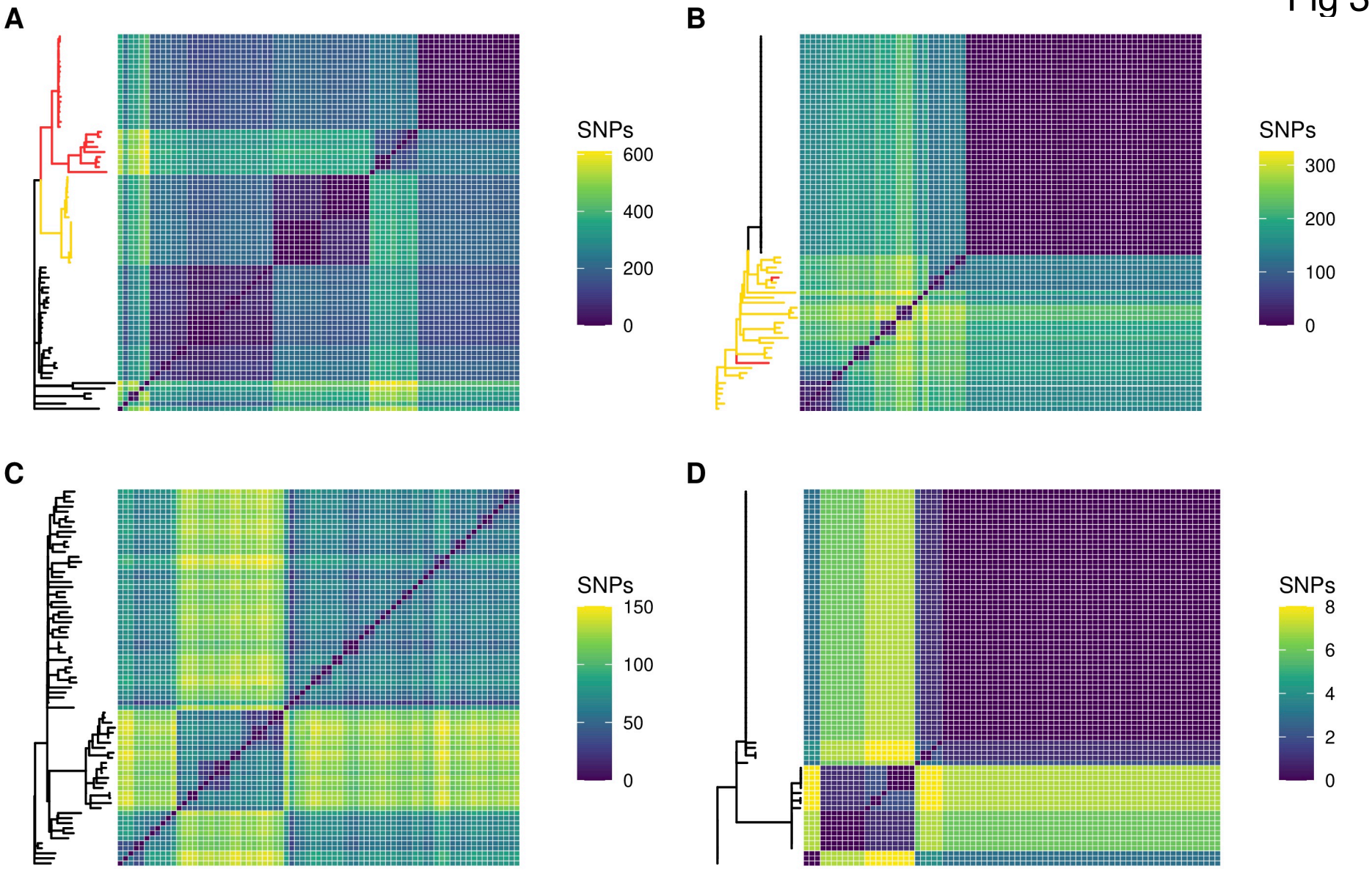
A
SNPs
600
400
200
0
B
SNPs
300
200
100
0
C
SNPs
150
100
50
0
D
SNPs
8
6
4
2
0

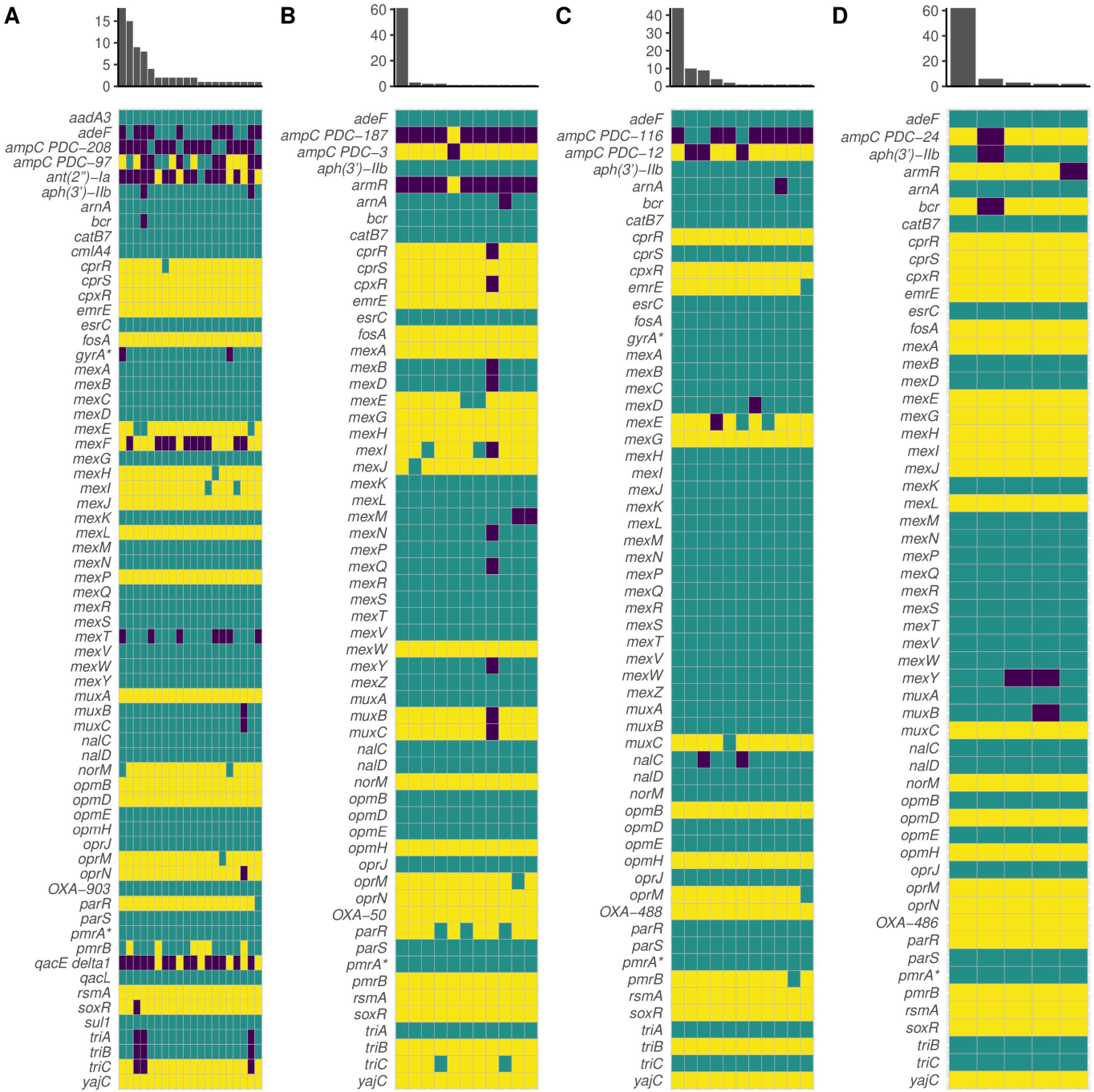
A
B
C
D
aadA3
adeF
ampC PDC−208
ampC PDC−97
ant(2")−Ia
aph(3')−IIb
arnA
bcr
catB7
cmlA4
cprR
cprS
cpxR
emrE
esrC
fosA
gyrA*
mexA
mexB
mexC
mexD
mexE
mexF
mexG
mexH
mexI
mexJ
mexK
mexL
mexM
mexN
mexP
mexQ
mexR
mexS
mexT
mexV
mexW
mexY
muxA
muxB
muxC
nalC
nalD
norM
opmB
opmD
opmE
opmH
oprJ
oprM
oprN
OXA−903
parR
parS
pmrA*
pmrB
qacE delta1
qacL
rsmA
soxR
sul1
triA
triB
triC
yajC
adeF
ampC PDC−187
ampC PDC−3
aph(3')−IIb
armR
arnA
bcr
catB7
cprR
cprS
cpxR
emrE
esrC
fosA
mexA
mexB
mexD
mexE
mexG
mexH
mexI
mexJ
mexK
mexL
mexM
mexN
mexP
mexQ
mexR
mexS
mexT
mexV
mexW
mexY
mexZ
muxA
muxB
muxC
nalC
nalD
norM
opmB
opmD
opmE
opmH
oprJ
oprM
oprN
OXA−50
parR
parS
pmrA*
pmrB
rsmA
soxR
triA
triB
triC
yajC
adeF
ampC PDC−116
ampC PDC−12
aph(3')−IIb
arnA
bcr
catB7
cprR
cprS
cpxR
emrE
esrC
fosA
gyrA*
mexA
mexB
mexC
mexD
mexE
mexG
mexH
mexI
mexJ
mexK
mexL
mexM
mexN
mexP
mexQ
mexR
mexS
mexT
mexV
mexW
mexZ
muxA
muxB
muxC
nalC
nalD
norM
opmB
opmD
opmE
opmH
oprJ
oprM
OXA−488
parR
parS
pmrA*
pmrB
rsmA
soxR
triA
triB
triC
yajC
adeF
ampC PDC−24
aph(3')−IIb
armR
arnA
bcr
catB7
cprR
cprS
cpxR
emrE
esrC
fosA
mexA
mexB
mexD
mexE
mexG
mexH
mexI
mexJ
mexK
mexL
mexM
mexN
mexP
mexQ
mexR
mexS
mexT
mexV
mexW
mexY
muxA
muxB
muxC
nalC
nalD
norM
opmB
opmD
opmE
opmH
oprJ
oprM
oprN
OXA−486
parR
parS
pmrA*
pmrB
rsmA
soxR
triB
triC
yajC

Fig 4

Fig 5

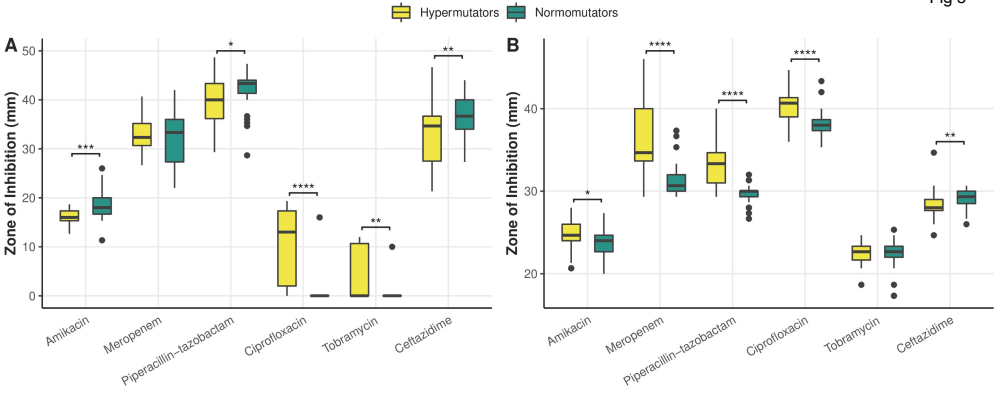
Hypermutators
Normomutators
A
B
Zone of Inhibition (mm)
Amikacin
Meropenem
Piperacillin–tazobactam
Ciprofloxacin
Tobramycin
Ceftazidime
***
*
****
**
*
****
****
****
**

Fig 6

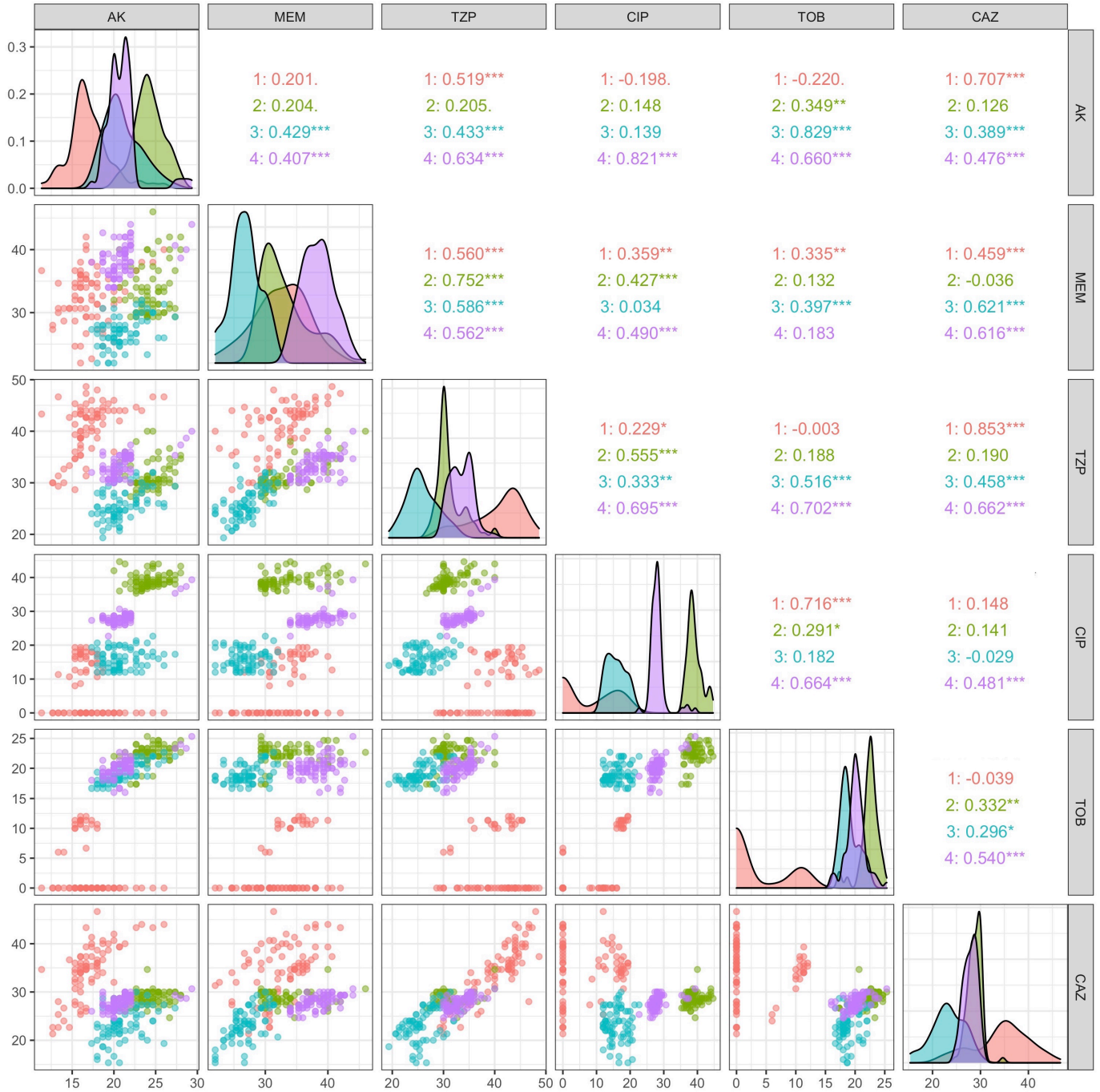
AK
MEM
TZP
CIP
TOB
CAZ
1: 0.201.
2: 0.204.
3: 0.429***
4: 0.407***
1: 0.519***
2: 0.205.
3: 0.433***
4: 0.634***
1: -0.198.
2: 0.148
3: 0.139
4: 0.821***
1: -0.220.
2: 0.349**
3: 0.829***
4: 0.660***
1: 0.707***
2: 0.126
3: 0.389***
4: 0.476***
1: 0.560***
2: 0.752***
3: 0.586***
4: 0.562***
1: 0.359**
2: 0.427***
3: 0.034
4: 0.490***
1: 0.335**
2: 0.132
3: 0.397***
4: 0.183
1: 0.459***
2: -0.036
3: 0.621***
4: 0.616***
1: 0.229*
2: 0.555***
3: 0.333**
4: 0.695***
1: -0.003
2: 0.188
3: 0.516***
4: 0.702***
1: 0.853***
2: 0.190
3: 0.458***
4: 0.662***
1: 0.716***
2: 0.291*
3: 0.182
4: 0.664***
1: 0.148
2: 0.141
3: -0.029
4: 0.481***
1: -0.039
2: 0.332**
3: 0.296*
4: 0.540***

Table 1. Metadata on the four patients in our cohort: sex, cystic fibrosis transmembrane conductance regulator (CFTR) mutation status, length of *P. aeruginosa* infection, clinical status, forced expiratory volume (% FEV1), modulator therapy, antibiotic treatment, and dominant infection strain type.

	Patient 1	**Patient 2**	**Patient 3**	**Patient 4**
Patient Sex	F	F	F	M
CFTR Mutation	F508del/R1162X	F508del/F508del	F508del/L467P	F508del/ 621+1G->T
Length of *Pa* infection	15 years, 2 months	12 years, 5 months	10 years, 4 months	13 years
Clinical status	APE Outpatient	APE Outpatient	Stable	APE Outpatient
FEV_1 (%)	67.96%	74.92%	67.83%	60.30%
Modulator Therapy	None	None	None	None
Antibiotic Treatment	Inhaled tobramycin, oral azithromycin	Inhaled tobramycin, oral Trimethoprim / Sulfamethoxazole	Inhaled tobramycin, inhaled aztreonam, oral azithromycin	Inhaled tobramycin, oral Trimethoprim / Sulfamethoxazole, oral levofloxacin
Dominant ST	870	2999	1197	274

Table 2. Genetic variations in each population: single nucleotide polymorphisms (SNPs), multiple nucleotide polymorphisms (MNPs), and insertions and deletions (indels).

	Patient 1	Patient 2	Patient 3	Patient 4
Total # unique SNPs/ MNPs	4592	1972	1638	31
# SNPs/ MNPs separating most divergent isolates	611	326	150	8
Non-synonymous SNPs/ MNPs	2803	1294	1024	24
Synonymous SNPs/ MNPs	1248	484	425	5
SNPs in non-coding regions	541	194	189	2
Total # indels	498	307	330	14
Indels in non-coding regions	204	99	115	2

Fig S1

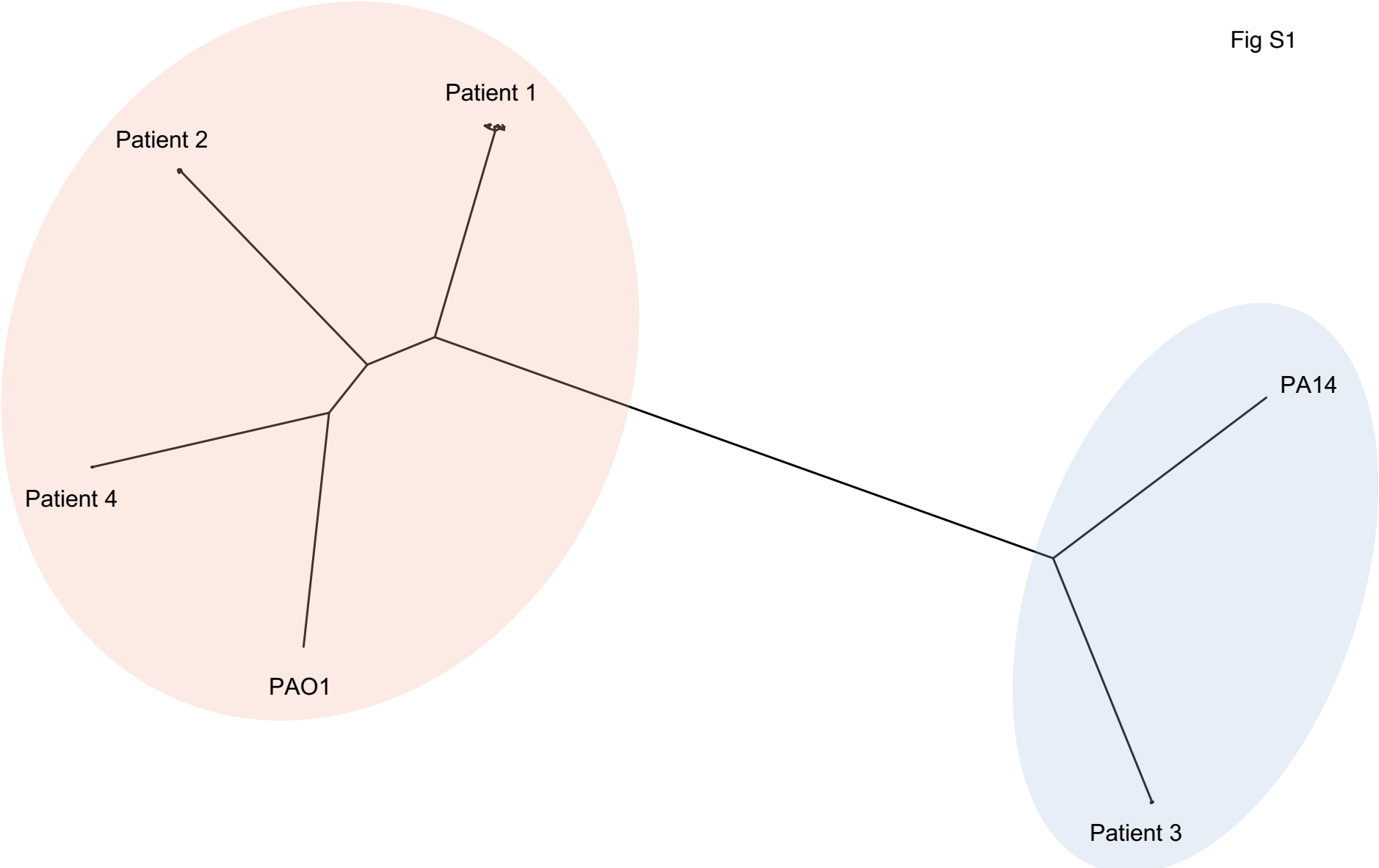

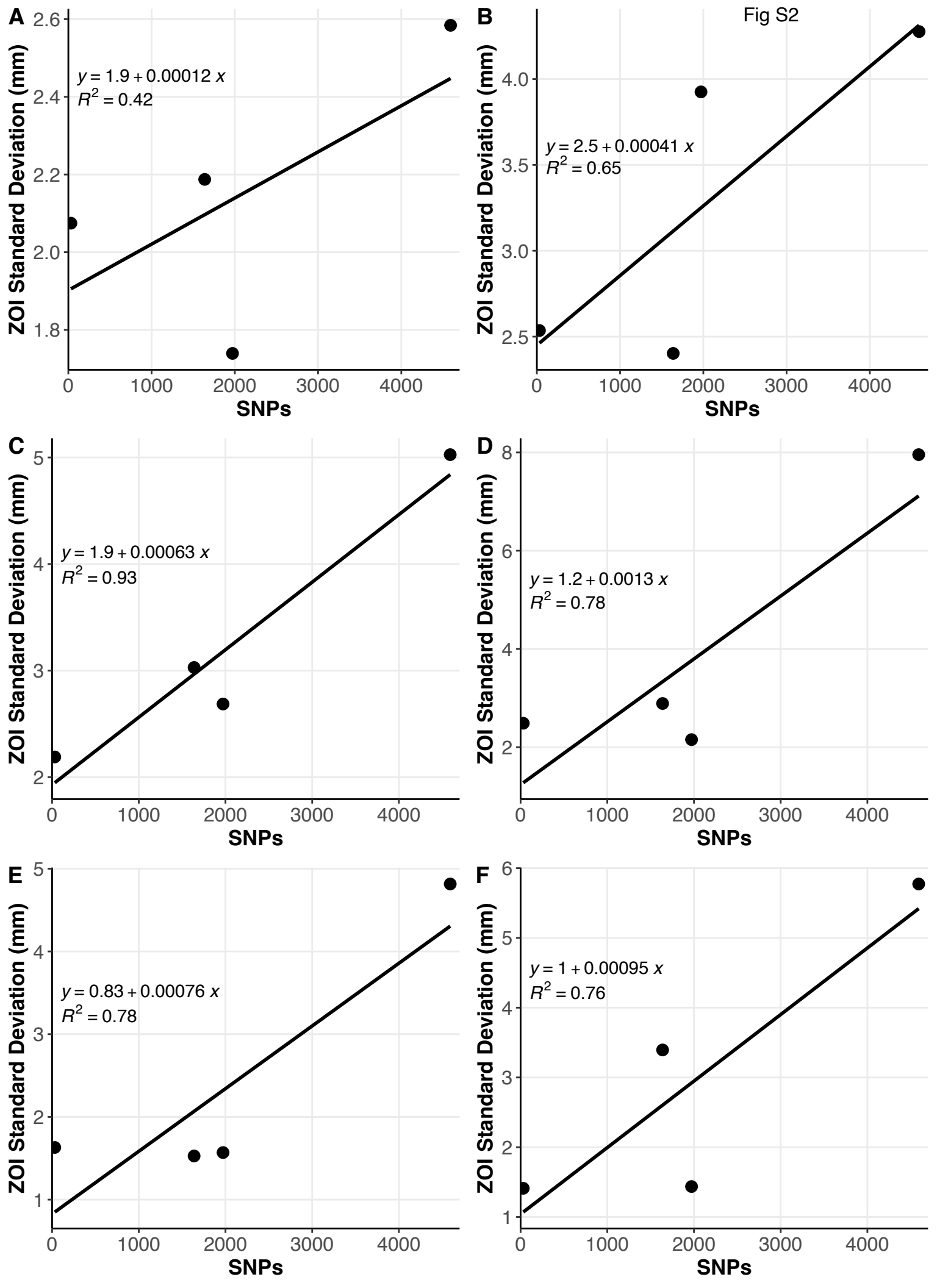
Fig S2
A
y = 1.9 + 0.00012 x
R2 = 0.42
B
y = 2.5 + 0.00041 x
R2 = 0.65
C
y = 1.9 + 0.00063 x
R2 = 0.93
D
y = 1.2 + 0.0013 x
R2 = 0.78
E
y = 0.83 + 0.00076 x
R2 = 0.78
F
y = 1 + 0.00095 x
R2 = 0.76
ZOI Standard Deviation (mm)
SNPs

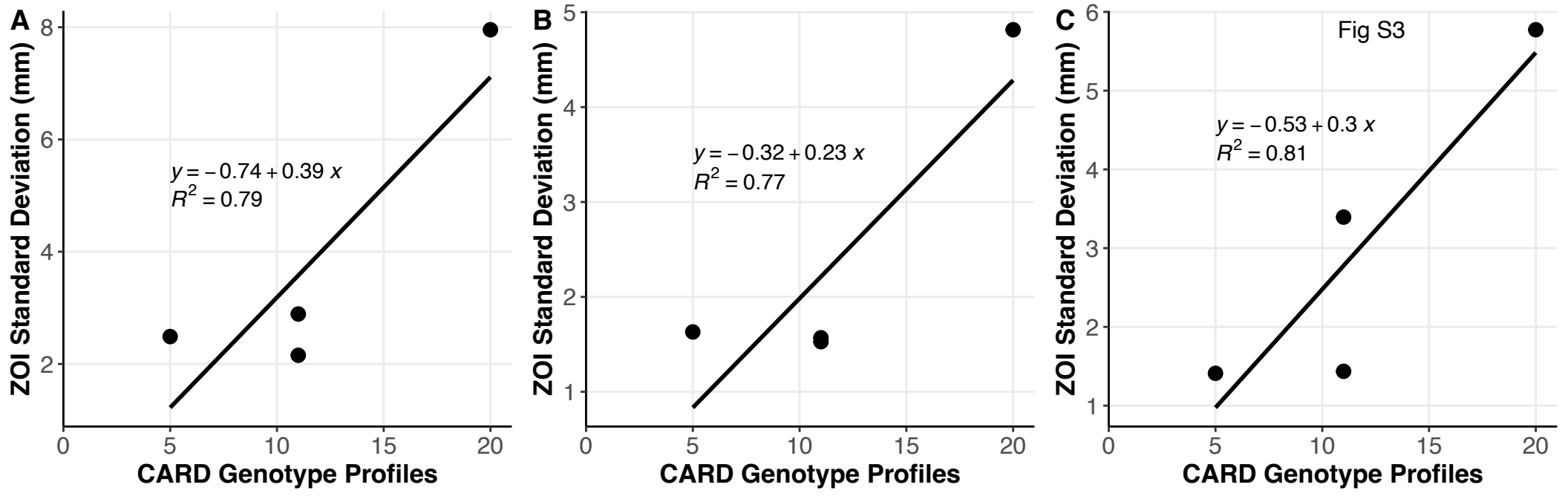
A
B
C
Fig S3
ZOI Standard Deviation (mm)
CARD Genotype Profiles
$y = -0.74 + 0.39\,x$
$R^2 = 0.79$
$y = -0.32 + 0.23\,x$
$R^2 = 0.77$
$y = -0.53 + 0.3\,x$
$R^2 = 0.81$

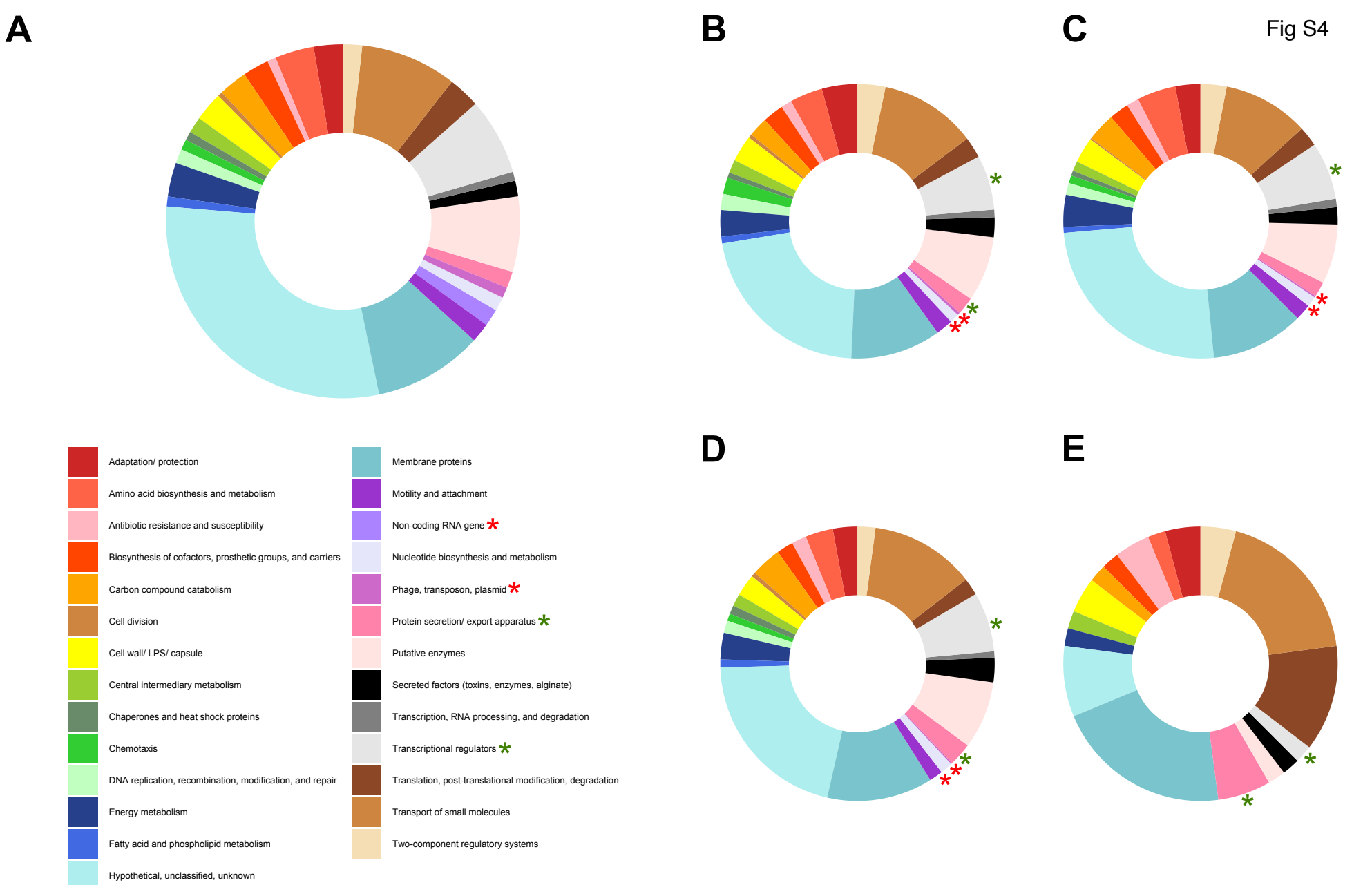
A
B
C
Fig S4
D
E
Adaptation/ protection
Amino acid biosynthesis and metabolism
Antibiotic resistance and susceptibility
Biosynthesis of cofactors, prosthetic groups, and carriers
Carbon compound catabolism
Cell division
Cell wall/ LPS/ capsule
Central intermediary metabolism
Chaperones and heat shock proteins
Chemotaxis
DNA replication, recombination, modification, and repair
Energy metabolism
Fatty acid and phospholipid metabolism
Hypothetical, unclassified, unknown
Membrane proteins
Motility and attachment
Non-coding RNA gene *
Nucleotide biosynthesis and metabolism
Phage, transposon, plasmid *
Protein secretion/ export apparatus *
Putative enzymes
Secreted factors (toxins, enzymes, alginate)
Transcription, RNA processing, and degradation
Transcriptional regulators *
Translation, post-translational modification, degradation
Transport of small molecules
Two-component regulatory systems

Fig S5

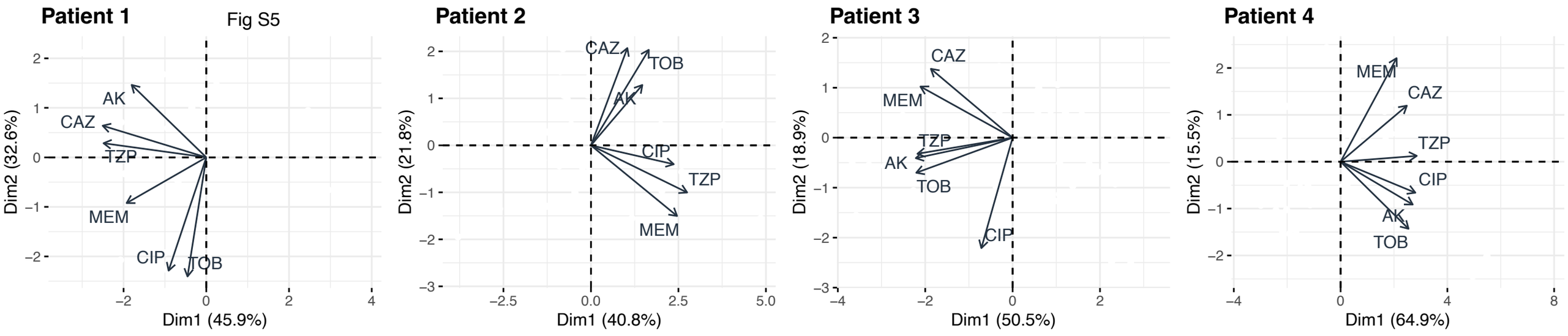
Patient 1
AK
CAZ
TZP
MEM
CIP
TOB
Dim2 (32.6%)
Dim1 (45.9%)
Patient 2
CAZ
TOB
AK
CIP
TZP
MEM
Dim2 (21.8%)
Dim1 (40.8%)
Patient 3
CAZ
MEM
TZP
AK
TOB
CIP
Dim2 (18.9%)
Dim1 (50.5%)
Patient 4
MEM
CAZ
TZP
CIP
AK
TOB
Dim2 (15.5%)
Dim1 (64.9%)

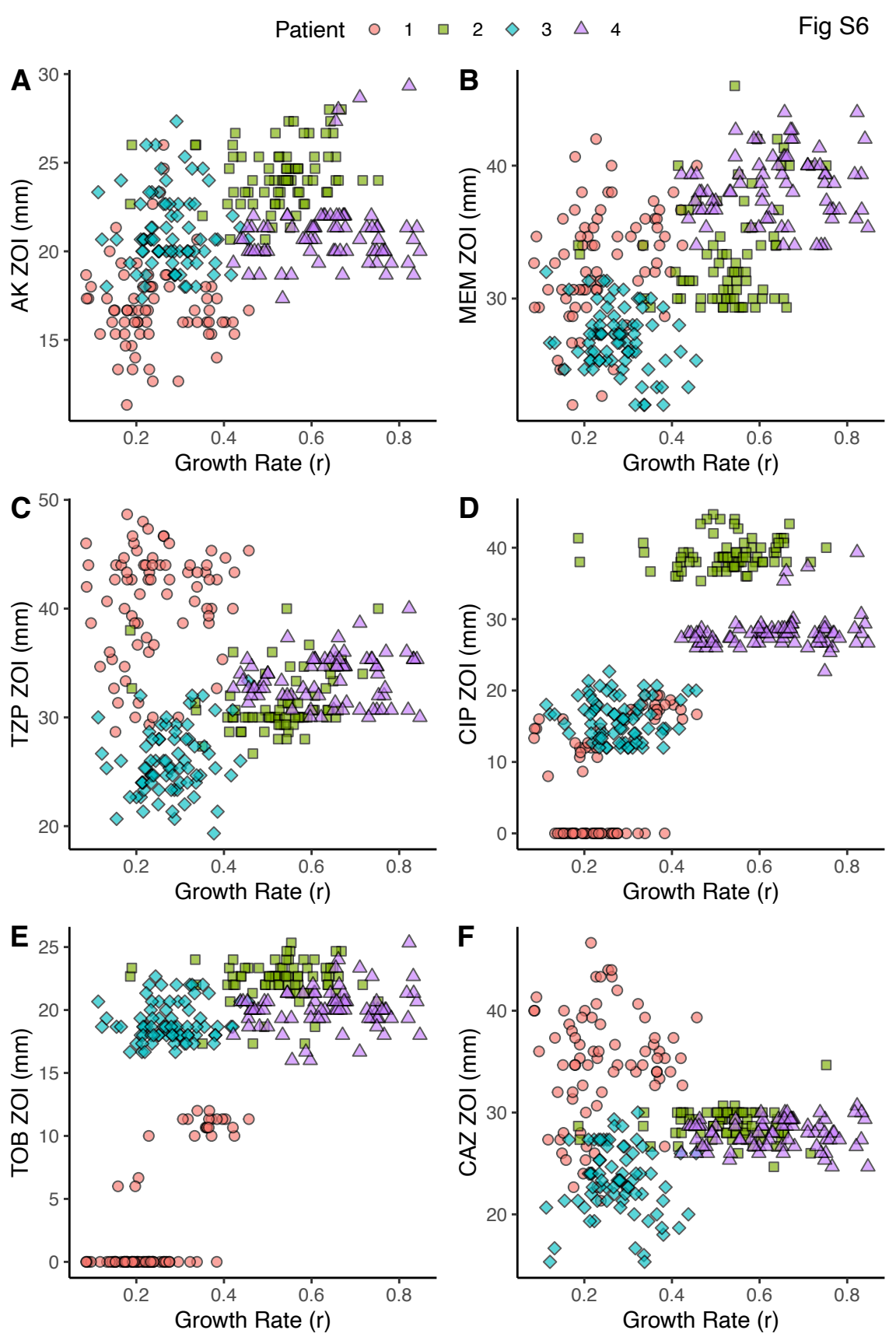
Patient 1 2 3 4
Fig S6
A
AK ZOI (mm)
Growth Rate (r)
B
MEM ZOI (mm)
Growth Rate (r)
C
TZP ZOI (mm)
Growth Rate (r)
D
CIP ZOI (mm)
Growth Rate (r)
E
TOB ZOI (mm)
Growth Rate (r)
F
CAZ ZOI (mm)
Growth Rate (r)